

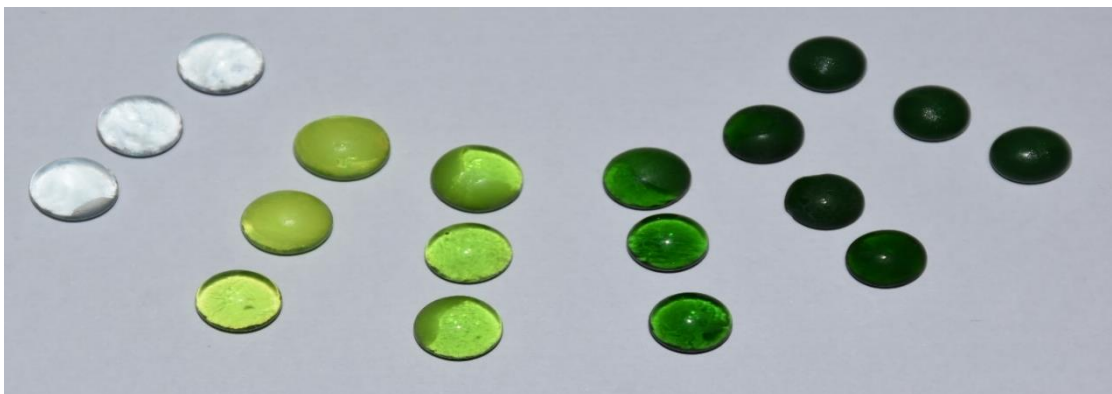
**SYNTHESIS AND
CHARACTERISATION OF CHROMIUM
OXIDE DOPED BIOACTIVE GLASS**

M.Sc. Physics Project Dissertation

Uttam Shirodkar and Aatish Dhargalkar

Guide: Dr. Reshma Raut Dessai

**School of Physical and Applied Sciences,
Goa University, Taleigao Plateau
May 2022**



| | |
|--|--------------|
| 1. CHAPTER 1: INTRODUCTION AND OBJECTIVE | 1-11 |
| 1.1. Introduction | 1 |
| 1.2. Amorphous materials and Crystalline material | 2 |
| 1.3. Glass..... | 2 |
| 1.3.1. Definition of Glass | 2 |
| 1.3.2. Methods of glass preparation..... | 3 |
| 1.3.3. Structure of glass..... | 3 |
| 1.4. Phase Transition..... | 5 |
| 1.4.1. Glass transition..... | 5 |
| 1.4.2. Volume temperature relation..... | 6 |
| 1.5. Bioactive glass..... | 7 |
| 1.5.1. Bioactivity in glass..... | 8 |
| 1.5.2. Mechanism of bioactivity..... | 9 |
| 1.6. Objectives of Present work..... | 10 |
| 2. CHAPTER II: EXPERIMENTAL TECHNIQUES | 12-23 |
| 2.1.1 Methods of glass preparation..... | 12 |
| 2.1.2 Preparation of Simulated body fluid (SBF)..... | 12 |
| 2.2. Xray Diffraction | 13 |
| 2.2.1. Principle..... | 14 |
| 2.2.2. Bragg's law | 15 |
| 2.3. Scanning Electron Microscopy and Energy Dispersive Spectrum..... | 17 |
| 2.3.1 Principle | 17 |
| 2.3.2 Working of SEM | 17 |
| 2.4. Fourier Transform Infrared Spectroscopy..... | 19 |

| | | |
|-------------|---|--------------|
| 2.4.1 | The Physics of Fourier Transform Infrared Spectrophotometer..... | 20 |
| 2.4.2. | Advantages of Fourier Transform Infrared Spectroscopy | 21 |
| 2.4.3. | Sample preparation for IR | 22 |
| 2.5. | Differential thermal analysis (dta)/thermogravimetric analysis (tg) | 23 |
| 3. | CHAPTER III: OBSERVATION AND DATA INTERPREPATION | 24-55 |
| 3.1. | Preparation of glass | 24 |
| 3.2. | Characterisation, Data Interpretation and results | |
| 3.2.1 | Density measurements on glass Sample beads | 29 |
| 3.2.2 | X ray diffraction | 30 |
| 3.2.3 | IR spectroscopy | 35 |
| 3.2.4 | SEM EDS | 39 |
| 3.2.5 | Thermogravimetric analysis | 45 |
| 3.3. | In vitro study of Bioactive glass..... | 46 |
| 3.3.1. | Preparation of SBF solution and loading in the glass compacts | 46 |
| 3.3.2. | XRD on Bio glass after immersion of glass tablets in SBF | 47 |
| 3.3.3. | SEM and EDS after immersion of glass tablets in SBF solution | 52 |
| 4. | CHAPTER IV: SUMMARY AND CONCLUSIONS..... | 56-57 |
| 5. | BIBLIOGRAPHY..... | 58-59 |

LIST OF FIGURES

| Figure # | Title | Page # |
|-----------------|--|---------------|
| 1 | Schematic 2D representation of amorphous compounds | 4 |
| 2 | Volume temperature behaviour of glass | 7 |
| 3 | Depiction of the integration of bioactive glass with bone | 10 |
| 4 | Experimental set up for preparation of simulated body fluid | 13 |
| 5 | Schematic representation of electromagnetic spectrum | 14 |
| 6 | Schematic representation of Bragg's law (condition for diffraction) | 15 |
| 7 | Rigaku smart lab X-ray Diffractometer. | 16 |
| 8 | SEM Instrument | 18 |
| 9 | Gold coating of sample tablet | 18 |
| 10 | Infrared spectrophotometer - Prestige-21 | 19 |
| 11 | Schematic representation of Michelson interferometer | 20 |
| 12 | Temperature and time relation graph for Sample A (0% Cr ₂ O ₃) | 26 |
| 13 | Temperature and time relation graph for Sample B (0.05% Cr ₂ O ₃) | 26 |
| 14 | Preparation of Glass samples | 27 |
| 15 | Preparation of glass samples | 27 |
| 16 | Prepared Glass samples | 28 |

| | | |
|----|--|----|
| 17 | Glass beads of various percentages of Cr ₂ O ₃ | 28 |
| 18 | X-ray spectrum of sample A | 31 |
| 19 | X-ray spectrum of sample B | 31 |
| 20 | X-ray spectrum of sample C | 32 |
| 21 | X-ray spectrum of sample D | 32 |
| 22 | X-ray spectrum of sample E | 33 |
| 23 | X-ray spectrum of sample F | 33 |
| 24 | X-ray spectrum of all samples clubbed together | 34 |
| 25 | IR spectrum of sample A, B & C | 37 |
| 26 | IR spectrum of sample D, E & F | 38 |
| 27 | SEM images of sample A, B & C | 40 |
| 28 | SEM images of sample D, E & F | 41 |
| 29 | Eds data of sample A B & C | 42 |
| 30 | Eds data of sample A B & C | 43 |
| 15 | Preparation of glass samples | 27 |
| 16 | Prepared Glass samples | 28 |

CHAPTER 1: INTRODUCTION AND OBJECTIVE

1.1. Introduction

For several years glass has been a topic of interest by many scientists due to its unique properties structurally chemically, biologically and also due to its mesmerising beauty. A study of physical properties of glasses is of utter importance as its insight gives us the fundamental working of them. The propelling desire towards the research of glasses is mainly due to scientific and technological excavations in the development towards its applications and for improved lifestyle of the human race. In past few years there have been immense progress in the development of bio-materials and functional materials having biological applications. Glass and glass ceramics have been used in bone replacement, osteogenesis and also in dental treatment. The bone-bonding ability of a material is often evaluated by examining the ability of apatite formation on its surface in a simulated body fluid (SBF) with ion concentrations nearly equal to those of human blood plasma. Tissues which are damaged can be restored by using scaffolds of engineering bio materials. Biomaterials are biocompatible and have several clinical applications and are currently being used as bone grafts, scaffolds and in dental implants [1]. Bioactive glasses are among the few most promising biomaterials in bone regeneration due to their ability to enhance enzyme activity [1,2]. Glass materials that can chemically bond with tissues are called bioactive glasses which exhibit osteoconductive properties [2]. Bioactive glasses are silicate based containing calcium and phosphates. Biomaterials have wide applications in many areas of medicine and human body part replacement such as bone, heart valve etc. that need to be improved by the use of nano-biomaterials. Study of Biomaterials involves multidisciplinary

science, i.e.; applicatory science and engineering science. Biocompatibility is the ability of a material to perform with an appropriate host response in a specific application [3]. Materials used in the replacement of tissues have come a long way from being compatible to regenerative. Earlier, Hydroxyapatite was believed to be the best biocompatible replacement material. Larry Hench developed bioactive material with silica as host incorporated with calcium and phosphorous, this mimics bone and stimulates regrowth of new bone material [3,4]. When this material is in contact with the tissues or body fluid, it develops a layer at the surface resulting in chemical bond between tissue and the implant [5]. In addition to compositional property such materials require to have a 3D interconnected porous structure to allow cell attachment and provide pathway for bio fluids.

1.2. Amorphous materials and Crystalline material

Crystalline solids have a definite and periodic geometry and they consist of long-range order for their constituent particles. Where as in case of amorphous solids they are arranged in an irregular manner and they don't really have any sort of definite geometry and they have only short-range order. In terms of melting point crystalline solids have a high and distinct melting points whereas in case of the amorphous solids they do not possess any sharp melting points. Crystalline solids are known to be the true solids where as amorphous solids are known to be pseudo solids. Crystalline solids tend to show anisotropy i.e., they have different properties when measured along different directions all axes whereas the same cannot be said for the amorphous solids as they show isotropy [6].

1.3. Glass

1.3.1. Definition of Glass

In 1930, glass was defined as an amorphous solid, i.e., a structureless solid. In 1949, American Society for Testing Materials (ASTM) defined glass as an inorganic product of fusion which is cooled to a rigid condition without crystallization [7]. But this definition was too restrictive as many organic glasses are known and fusion is not only the method to make glass. Later in 1968, glass was redefined as an amorphous solid which exhibits a glass transition. A glass can be defined as “Amorphous solid completely lacking in long range, periodic atomic structure and exhibiting a region of glass transformation behavior” [8].

1.3.2. Methods of glass preparation

Glasses are formed by abrupt cooling from a melt i: e. they are supercooled. One can form glasses by vapour deposition, sol-gel processing or say by melt quenching method. Historically glasses are inorganic and non-metallic.

1.3.3. Structure of glass

By structure it is referred to a precise description of the substance in terms of atomic positions, bond lengths and bond angles. In any case of a crystal the arrangement of the atoms or ions is periodic. The detailed description of such a structure is complete once the dimensions and the content of the unit cell are uniquely specified. The position of all atoms is then determined by translation of such cell along the three directions of space. Crystals usually possess both, a short- and long-range order and the crystallographic methods, are based on the properties of point groups and translational groups which characterize a given structure. The case of disordered materials such as glasses and liquids are more intricate. Only short-range and medium range order is present and the unit cell can't be defined. The most important theory which influenced glass science was given by the Norwegian-American physicist William Zachariasen.

He basically considered the relative glass-forming ability of simple oxides and concluded that the ideal condition for glass formation is that the material should be capable of forming an extended three-dimensional network structure without any long-range order [9].

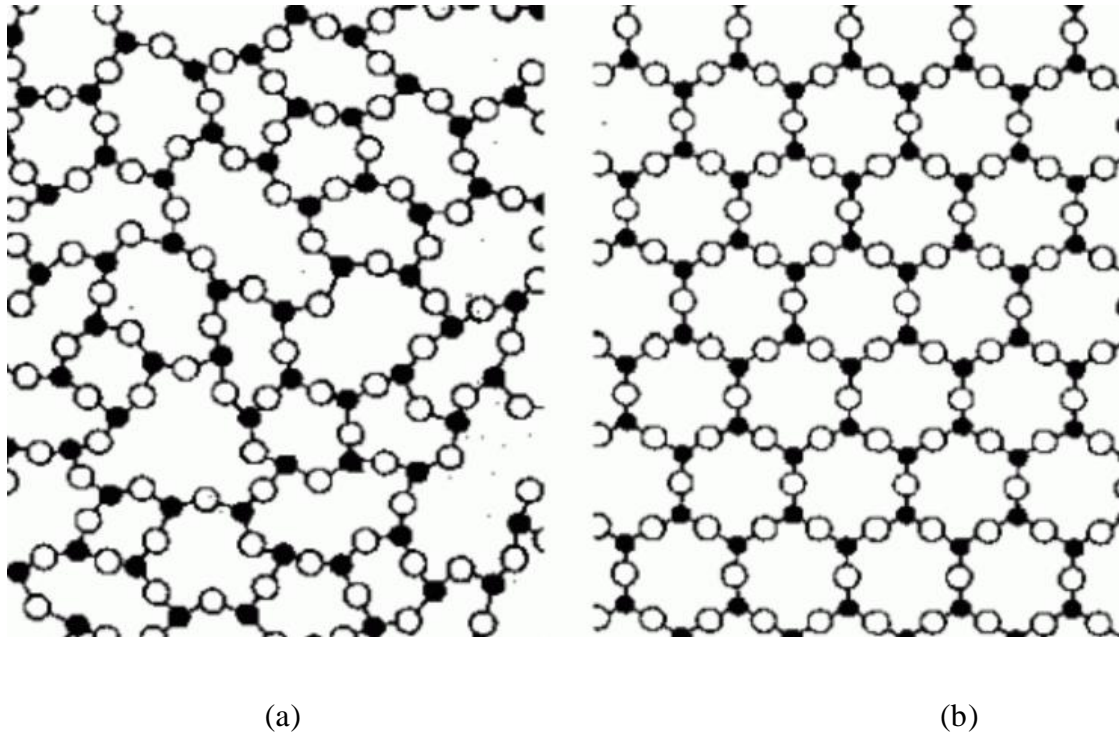


Figure 1: Schematic 2D representation of (a) Amorphous and (b) Crystalline compound

For a glass made up of silicon dioxide (SiO_2) the crystalline form of silica contains SiO_4 tetrahedra joined at the corners of the structure. Glassy silica must also contain SiO_4 tetrahedra joined at respective corners. Zachariasen formulated a set of empirical rules known as Zachariasen's rules which an oxide must satisfy, which are as follows:

1. No oxygen atom might be linked to more than two atoms.
2. The number of oxygen atoms surrounding any given atom should be small.
3. The oxygen polyhedra share corners with each other and not edges or even faces.

4. The polyhedra link-up to form a three-dimensional network. i.e., at least three corners of each polyhedron should be shared [10].

Oxides like SiO_2 , B_2O_3 , GeO_2 , etc. satisfy these empirical rules and are good glasses in forming oxides.

1.4. Phase Transition

Phase transition is a phenomenon in which a given material changes its state from one form to another. In case of transition of glasses an amorphous-solid changes its state from solid to supercooled liquid with abrupt changes in its derivative thermodynamic properties.

Whenever any liquid is cooled from a certain high temperature, crystallization may take place at a melting point which is T_m . If crystallization occurs, there will be a sudden change in the volume at T_m . Should the crystallisation arise, there will be a sudden change in the volume at T_m , and hence the glass formation typically takes place and thus there will be a gradual alteration in the slope. The region over which this alteration occurs is known as temperature T_g which is known as glass transition temperature [11]. This is explained in the figure below:

1.4.1. Glass transition

A given liquid when cooled, either crystallizes at the melting temperature or liquid could become super cooled for temperatures below melting temperature. The glass-liquid transition or glass transition is the reversible transition in amorphous materials from a hard and relatively brittle "glassy" state into a viscous state as the temperature is risen. The reverse transition which is achieved by supercooling a viscous liquid into the glass state, is called vitrification [12]. Most of the inorganic compounds melt to

form liquid and when such liquids are cooled, rapid crystallisation takes place at the melting point.

1.4.2. Volume temperature relation

The volume temperature relation is shown in figure below. As the temperature of the liquid decreases from the starting point 'a' the volume of the given mass decreases along 'ab'. If the rate of cooling is low and nuclei are present in melt, crystallization will take place at the temperature T_m , accompanied by decrease in volume along line 'bc'. On further cooling the crystalline material contracts along the trend 'cd'. Whereas if the rate of cooling is appreciably high, crystallization does not take place at ' T_f '. As the cooling continues the volume of now super cooled liquid decreases along line 'be' which is a smooth continuation of 'ab'. At a certain temperature T_g , the volume temperature curve of the super cooled liquid undergoes a marked change in the direction and continues almost parallel to the contraction curve of the crystalline state. This range of temperature over which the slope changes is called the glass transition temperature T_g . Between T_g and T_f , the material is a super cooled liquid. The difference between supercooled liquid and glass can be understood by considering what happens when temperature of glass is held constant at T , which is below T_g . It is found that the volume decreases slowly until it eventually reaches a point on the dotted line, which is a smooth continuation of contraction curve of the supercooled liquid. This process by which a glass reaches more stable condition is known as stabilization. Above T_g no such time dependence is observed. Without crystallization the supercooled liquid cannot achieve a more stable condition. Given a sufficiently long period of time, glass can achieve more stability at a temperature well below T_g [13]. The properties of a given composition

of glass depends to a certain extent on the rate at which it has been cooled through the temperature range near T_g . The precise value of T_g depends on the rate of cooling. However, T_g is an indicator of the approximate temperature where the super cooled liquid converts to a solid on cooling.

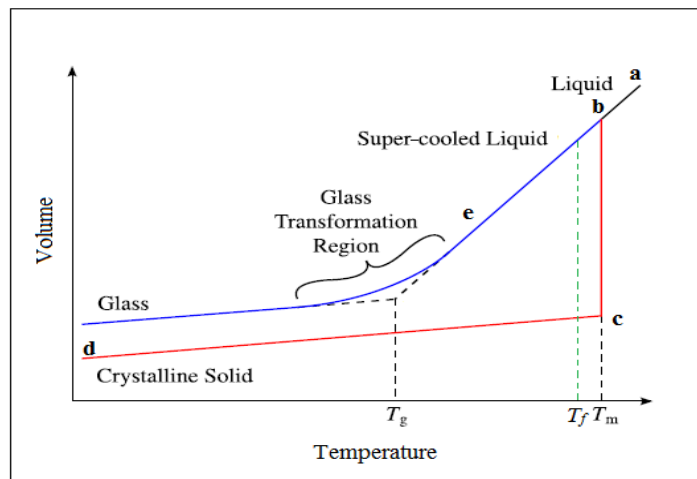


Figure 2: Volume temperature behaviour of glass

1.5. Bioactive glass

There has been immense progress in the development of bio-materials and functional materials with bio-applications. Glasses are among the most ancient of materials used by humans in multiple forms, with applications ranging from common household materials to technical fields. Bioactive glass is used for bone replacement therapy. Bio glasses dissolve in the body fluid or blood plasma present in our body and takes the place of bones, because of its composition stimulates bone and cell regeneration. Hydroxyapatite is considered to be the best biocompatible replacement material [4], he developed a material using silica as the host material, assimilate with calcium and phosphorous to bind broken bones [14]. Bioactive glasses are composed of calcium and phosphates which are present in a proportion that is similar to bone hydroxyapatite and

can bond to a tissue and stimulate new bone growth. They therefore have the potential to restore diseased or damaged bone to its original state. Its advantages include nontoxicity, biocompatibility, bioactivity, and bactericide capability. Glass has a non-crystalline structure which exhibits a glass transition when cooled from the liquid or super-cooled state to ambient temperature resulting in a rigid state on a macroscopic time scale. The structure of a glass affects its macroscopic properties such as stability, density, solubility and ion release in aqueous environment. Doping such materials with specific ions they can be made bio functional for specific applications.

1.5.1. Bioactivity in glass

The properties of these Bioactive glasses from the material technology point of view, the non-crystalline structure of these bioactive glasses offer the possibility of adjusting their physical and chemical properties by altering their oxide composition within certain limits and thus, understanding the relationships between the oxide composition and the relevant properties is essential when the glass composition is tailored for various product forms to be used in novel hard and soft tissue applications [15].

The surface modification of biomaterials has exhibited great potential in biological applications by transforming the existing surface into more appropriate compositions or topographies. The surface of bioactive glasses plays a vital role in their performance.

Bioactive glasses have unique properties that promote bone growth, and has often since been used in regenerative medicine as a material to replace bone or in dentistry. In addition, there has been a surge in interest recently in new applications for the material in soft tissue [16/17]. The approximate original glass composition in wt%

Table 1: Composition of first bioactive glass 45S5

| Compound | Weight % |
|----------|----------|
|----------|----------|

| | |
|-------------------------------|------|
| SiO ₂ | 45 |
| Na ₂ O | 24.5 |
| CaO | 24.5 |
| P ₂ O ₅ | 6 |

The glass composition of first glass composition as studied by Larry Hench was trade named 45S5 Bioglass. These biomaterials have minerals that are naturally occurring in the body i: e Silicon dioxide, calcium, sodium oxide and phosphorous dioxide. The composition of calcium and phosphorous oxide is similar to that of the bone. Once these bioglass implantation is carried out in the body it is subjected to body fluids and converts to a silica -CaO.P₂O₅ rich layer which subsequently mineralises into hydrocarbons in quick hours. Dissolution improves the bone tissue growth. Hydroxyapatite (HA) is a natural mineral form of calcium apatite. The chemical formula of hydroxyapatite is Ca₅(PO₄)₃(OH). HA like compounds contains about 65% of bone materials making it a good option for synthetic bone composite. HA can be synthesized by wet chemical deposition, sol gel method or biomimetic deposition.

1.5.2. Mechanism of bioactivity

The mechanism that enables bioactive glasses to clone as materials for bone repair have been investigated since the first work of Hench et al. at the University of Florida. Based on the observations it was the inquisitiveness of these materials that lead to changes in the bioactive glass surface. Five inorganic reaction levels are commonly thought to occur when a bioactive glass is immersed in a physiological environment [18].

1. Ion exchange in which along with modifier cations (mostly Na⁺) in the glass exchange with hydronium ions in the external solution.
2. Hydrolysis in which Si-O-Si bridges are broken, forming Si-OH silanol groups, and the glass network results in sudden disruption.

3. Condensation of silanols in which the disrupted glass network changes its morphology to form a gel-like surface layer which is depleted in sodium and calcium ions.
4. Precipitation in which an amorphous calcium phosphate layer is deposited on gel.
5. Mineralization in which the calcium phosphate layer slowly transforms into crystalline hydroxyapatite, that replicates the mineral phase naturally contained with vertebrate bones.

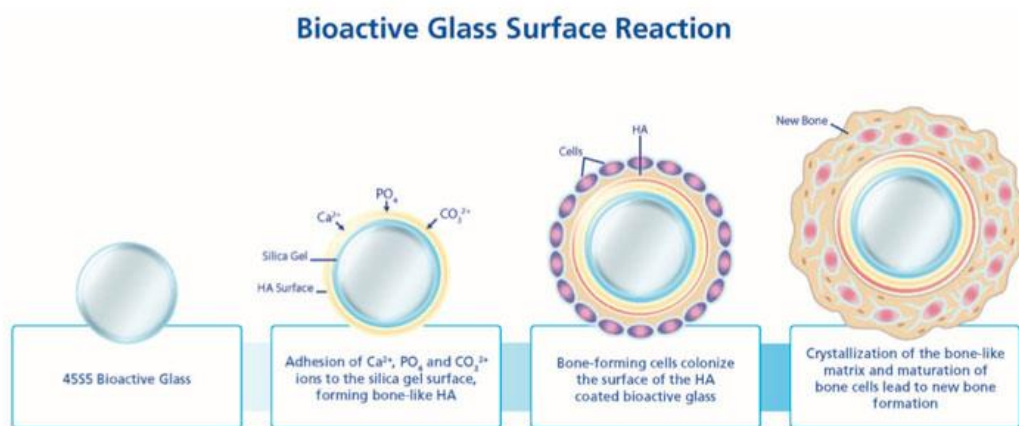


Figure 3: Depiction of the integration of bioactive glass with bone

Furthermore, it was discovered that the morphology of the gel surface layer was a key component in determining the bioactive response. This was backed up by studies on bioactive glasses derived from sol-gel processing. These glasses could contain significantly higher concentrations of SiO_2 than traditional melt-derived bioactive glasses and still maintain bioactivity i.e., the ability to form a mineralized hydroxyapatite layer on the surface. The inherent porosity of the sol-gel-derived material was cited as a possible explanation for why bioactivity was retained, and often improved with respect to the melt-derived glass [18/19].

1.6. Objectives of Present study

Investigation on bioactive glasses was done in long periods in mineralized tissue regeneration but the recent times have proved their potential applications in soft tissue repair and in particular with wound healing. Chromium in living organisms occurs as a trace element, yet its presence is extremely important. It coordinates the normal function of the body through proper metabolic transformations. The optimum level of chromium in the body allows for maintaining proper sugar level in the blood, normalizes cholesterol level, takes part in the metabolism of fats, proteins and carbohydrates, and reduces appetite. Due to its properties, chromium is used in the production of orthopaedic implants. There is still some concern regarding the local toxicity of chromium contained in prostheses [20]. The main objective of our field of research is to investigate the role of Cr with various percentages in the bioactive glass for the use of medical purposes, and to characterise it with various tests. To prepare simulated body fluid and test it for the glass samples prepared using xrd and SEM.

CHAPTER II: EXPERIMENTAL TECHNIQUES

2.1.1. Methods of glass preparation

The common methods used in the preparation of glass are Melt quenching method, Sol gel methods, Vapour decomposition method. In the present study the glasses with various composition of Cr_2O_3 were prepared using the well-known Melt quenching method. Melt quenching technique was the first glass preparation technique used in glass industry as well as in research field. Glasses with Cr_2O_3 composite system standard melt quenching technique was employed. Certain materials rapidly form glasses on cooling, but the chemical oxides do not have tendency to form glasses as the glass formation depends on the mixture of compounds. The factors that play vital role in signifying glass formation are the chemical or structural characteristics of glass system, thermodynamic or free volume aspects of the compounds. This method allows the flexibility of large number of compositions of glass of silicate, borate, phosphate, oxide or non-oxide systems. Also, the doping of other elements is easy with this method of preparing glass.

2.1.2. Preparation of Simulated body fluid (SBF)

A simulated body fluid (SBF) was first introduced by Kokubo et al. [21] to understand the changes on a surface of a bioactive glass ceramic. It is a solution with ion concentration similar to that of human blood plasma having identical physiological temperature. To prepare SBF glassware's are cleaned using 1 N HCL and dried in oven.

All required reagents are mixed. 500 ml of ion-exchanged and distilled water is placed in one liter polyethylene bottle and covered. Using magnetic stirrer all the content is stirred to dissolve the reagents pouring it one by one as given in the table (2). The process is carried out at 36.5°C in a water bath. Maintain the pH of solution to 7.40 by stirring the solution and titrating 1N HCL solution. The arrangement is as shown in the figure (4). Transfer the solution to volumetric glass flask. Adjust the volume to 1 litre by adding ion exchanged distilled water and shaking the flask at 20 °C. Transfer the solution in polyethene bottle and store in refrigerator at 5 to 10 °C.

Table 2: Reagents for preparing SBF

| Order | Reagent |
|-------|---|
| 1 | NaCl |
| 2 | NaHCO ₃ |
| 3 | KCl |
| 4 | K ₂ HPO ₄ · 3H ₂ O |
| 5 | MgCl ₂ · 6H ₂ O |
| 6 | 1M-HCl |
| 7 | CaCl ₂ |
| 8 | Na ₂ SO ₄ |
| 9 | (CH ₂ OH) ₃ CNH ₂ |

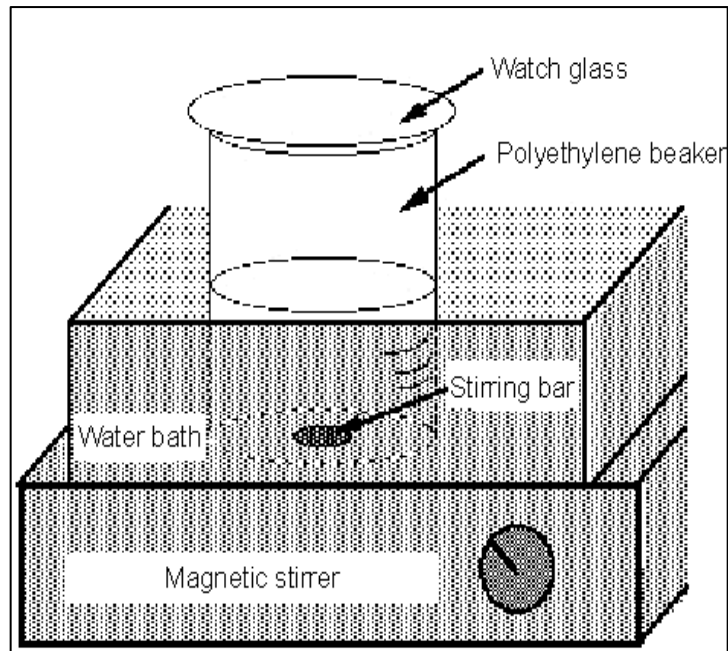


Figure 4: Experimental set up for preparation of simulated body fluid

2.2. X-ray Diffraction

X-ray is a nondestructive powerful technique used commonly for revealing the structure of crystalline materials. X-rays are electromagnetic waves of wavelength of about 1 Å, which is comparable to the atomic distances. In electromagnetic spectrum X-rays occupy the place in between gamma and ultraviolet rays as shown in figure (5).

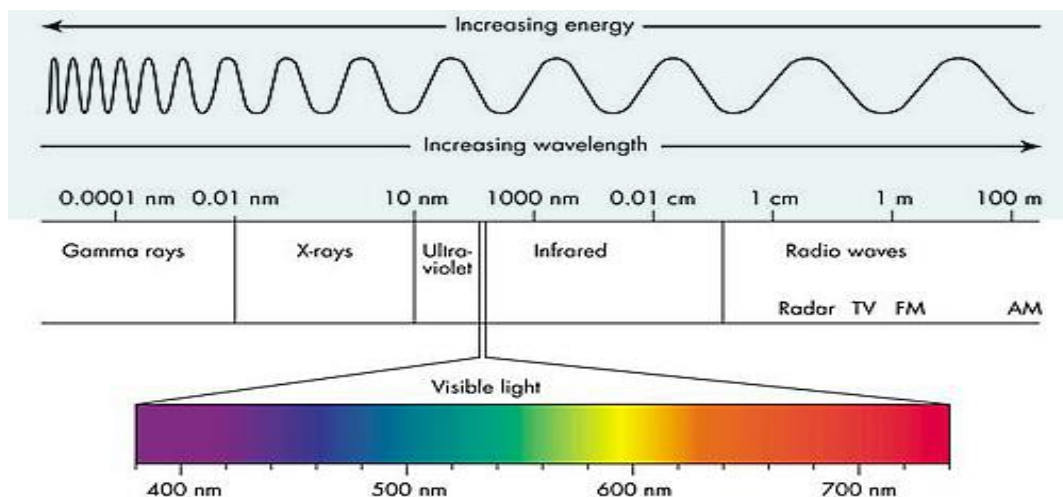


Figure 5: Schematic representation of electromagnetic spectrum

Diffraction is the phenomenon where there is bending of light over the edges of obstacle if the dimensions of the obstacle are comparable to the wavelength of waves.

X-ray diffractometers consist of three basic elements: an X-ray tube, a sample holder, and an X-ray detector. X-rays are generated in a cathode ray tube by heating a filament to produce electrons, accelerating the electrons toward a target by applying a voltage, and bombarding the target material with electrons.

2.2.1. Principle: When X-rays are incident on the uniformly spaced atoms in a crystal, the X-rays are diffracted by the electrons in the material. If the arrangement of atoms is regular pattern (crystalline material), scattering results in maxima and minima in the diffracted intensity [22]. The diffracted waves from the atomic planes of the crystals give rise to an interference pattern which gives information on the basic structure of the crystal. Each crystalline solid has its unique characteristic diffraction pattern.

The phenomenon of X-ray diffraction was identified by Von Laue in 1912. But the formulation that it was form of constructive interference and its utilization of identifying crystal lattices was done by William Lawrence Bragg's son of William Henry Bragg. Bragg's law gave interpretation to Laue's experiment on diffraction of X-ray by crystals.

2.2.2. Bragg's law: According to Bragg's law a monochromatic X-rays incident on a crystal is reflected from successive parallel planes of atoms in the crystal. The strong diffracted beams are obtained when the reflection from the parallel planes of atoms in the crystal interfere constructively [23]. Strong intensities known as Bragg peaks are obtained in the diffraction pattern when the maxima follow Bragg's condition

$$n\lambda = 2d\sin\theta \quad (1)$$

Where, $n = \text{integer}$,

$\lambda = \text{characteristic wavelength of the X-rays impinging on the sample}$,

$d = \text{interplanar spacing between rows of atoms}$,

$\theta = \text{angle of the X-ray beam with respect to these planes}$.

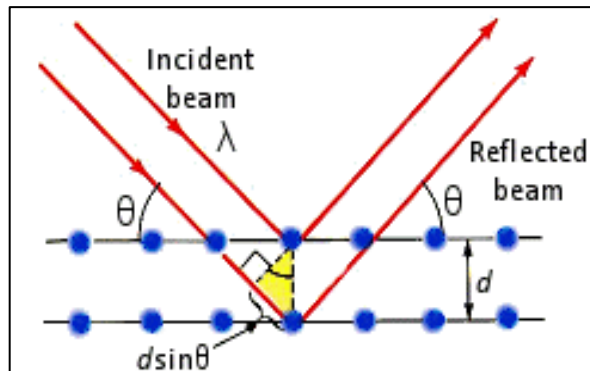


Figure 6: Schematic representation of Bragg's law (condition for diffraction)



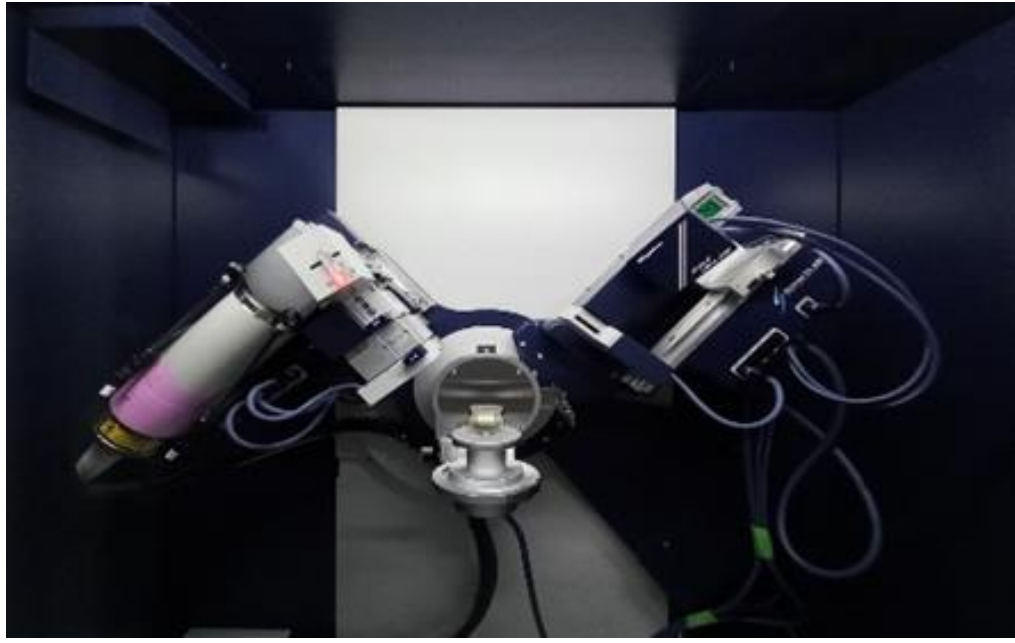


Figure 7: Rigaku smart lab Xray Diffractometer

2.3. Scanning Electron Microscopy (SEM) and Energy Dispersive Spectrum (EDS)

The scanning electron microscope (SEM) uses a focused beam of electrons with high energy to generate a signal at the surface of solid specimens. The signals that derive from electron-sample interactions give us information about the sample [24].

2.3.1 Principle:

The beam of electrons is generated by a suitable source, typically a tungsten filament or a field emission gun. The electron beam is accelerated through a high voltage and pass through a system of apertures and electromagnetic lenses to produce thin beam of electrons. Surface of the specimen is scanned by the beam. Electrons are emitted from the specimen by the action of the scanning beam and collected by a suitably positioned detector.

2.3.2. Working of SEM:

When tungsten wire is heated by passing current the electron gun produces an electron beam. The beam is accelerated by the anode and it travels through electromagnetic

fields and lenses, which focus the beam down towards the sample. The deflection coils guide the beam to scans the surface of the sample in a rectangular frame. When the beam touches the surface of the sample, secondary electrons (SE), back scattered electrons (BSE), and the X-rays are produced. These signals are collected by one or more detectors to form images which are then displayed on the computer screen. The scattered electron detector will collect the emitted scattered electrons and are converted into signal that is sent to a screen which produces a final image. The x-rays, back scattered electrons are collected by the additional detectors and produce corresponding images [25]. The main components of SEM are source of electrons, column-down which electrons travel with electromagnetic lenses, electron detector, sample chamber, computer and display to view the images. Electrons are produced at the top of the column, accelerated down, and passed through a combination of lenses and apertures to produce a focused beam of electrons which then strikes the surface of the sample. EDS makes use of the X-ray spectrum emitted by a solid sample bombarded with a focused beam of electrons to obtain a localized chemical analysis. Qualitative analysis involves the identification of the lines in the spectrum. Quantitative analysis entails measuring line intensities for each element in the sample and for the same elements in calibration Standards of known composition. The images produced by electrons collected from the sample reveal surface topography or mean atomic number differences according to the mode selected [25].



Figure 8: SEM Instrument

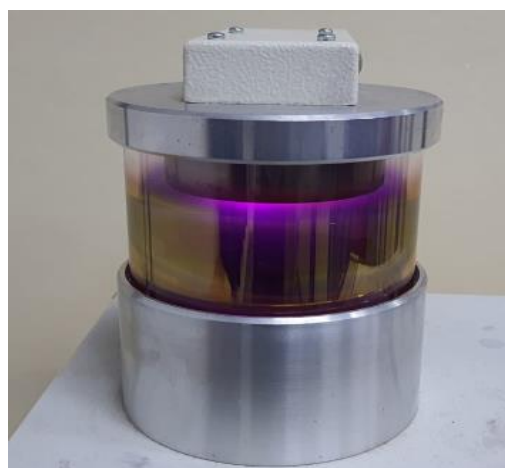


Figure 9: Gold coating of sample tablet

2.4. Fourier Transform Infrared Spectroscopy

Infrared absorption spectra can provide valuable information about the arrangement of atoms, nature of chemical bonds. The IR region on electromagnetic spectrum includes radiation at wavelengths between 0.7 and 500 microns extending from the red of the visible spectrum to the microwave region. Infrared spectrophotometry involves the twisting, bending, rotating and vibrational motion of atoms and molecules. All molecules are made up of atoms linked by chemical bonds. Upon interaction with atoms, a portion of the incident radiation is absorbed at a particular wavelength. The molecule will absorb certain frequencies as the energy is consumed in stretching or bending different bond. The multiplicity of vibrations occurring simultaneously

produces a highly complex absorption spectrum, which is uniquely characteristic of functional groups comprising the molecule and of the overall configuration of atoms as well. The transmitted beam corresponding to the region of absorption will be weakened. Thus, recording of intensity of the transmitted infrared beam v/s wavenumbers or wavelength will give a curve showing absorption bands which is the infrared spectra.



Figure 10: Infrared spectrophotometer - Prestige-21

By interpretation of the spectrum, we can find the functional group present in the material. The IR spectrum is the characteristic signatures of a compound. For the IR region of 10 cm^{-1} information obtained mainly of vibrations involving heavy atoms or bond distortions. Optical glass absorbs strongly in the IR and UV spectral regions. The former is associated with the interaction of light and molecular vibrations giving rise to multiphonon absorption processes while the latter is associated with electronic transitions between the valance band and conduction band.

2.4.1. The Physics of Fourier Transform Infrared Spectrophotometer

The FTIR works on a Michelson interferometer, after passing through the aperture, light is turned into a parallel beam by the collimator and enters the beam splitter. A schematic diagram of the interferometer is shown in (Fig 11).

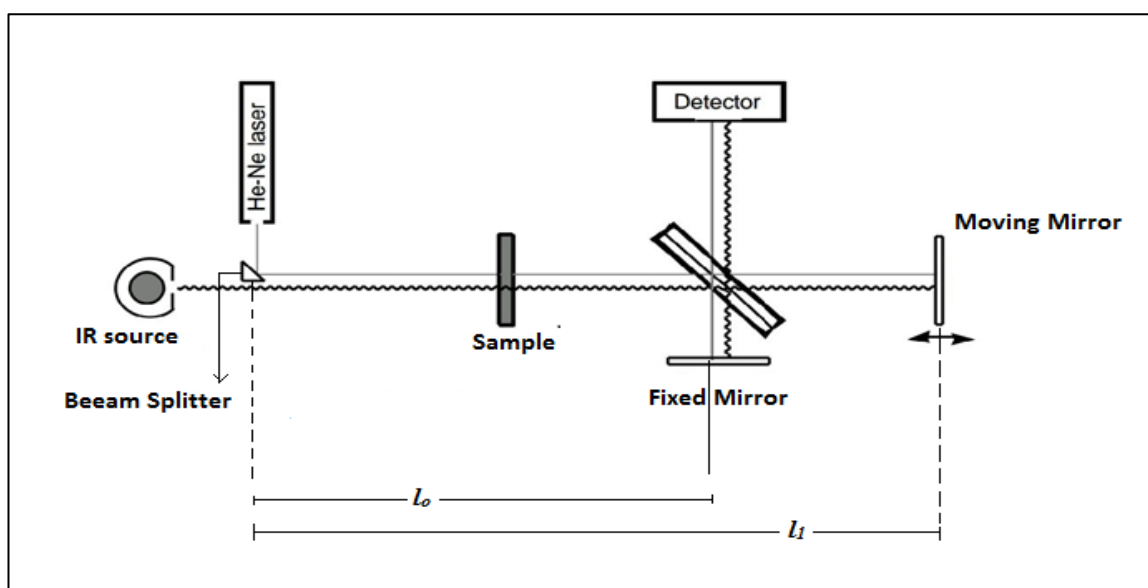


Figure 11: Schematic representation of Michelson interferometer

A germanium film, deposited on a KBr substrate via evaporation comprises the beam splitter, it splits the single beam into two. Reflecting one to the fixed mirror and transmitting the other to the moving mirror. Both mirrors reflect this beam back to the splitter, part of each returning beam is reflected and transmitted. The transmitted light from the fixed mirror and the reflected light from the moving mirror recombine and interfere with each other as they travel towards the collecting mirror. The interference is either constructive or destructive. FTIR optical system is shown in (Fig. 11).

Assume that the light source emits monochromatic light of wavelength λ (cm). When the distance between the fixed mirror and the beam splitter (l_0) is equal to the distance between the moving mirror and the beam splitter (l_1), the optical path difference between the two beams, $X=2(l_1 - l_0)$; is equal to zero, and the beams are in phase. While in phase, the beams interfere constructively with each other. As the mirror is displaced

by $\lambda/4$, the optical path difference becomes $\lambda/2$, and the two beams are out of phase, interfering destructively. Thus, the two beams interfere constructively with each other when $x=n\lambda$ and destructively when $x=(n + \frac{1}{2}) \lambda$ where n is an integer.

Equation below extrapolated from the above principles, calculates the intensity $I(x)$ of the length (wavelength) incident to the detector.

$$I(x) = 4RTS (\lambda) [1/2 + (1/2\cos (2\pi x))/I] \quad (2)$$

Where,

R–energy reflected by the beam splitter

T – Energy transmitted by the beam splitter

S (λ) – radiation energy from the light source

2.4.2. Advantages of Fourier Transform Infrared Spectroscopy

Because it is not necessary to scan each wave number successively, the whole spectrum is measured in at most few seconds. Because it is not dependent upon a slit and a prism or grating, high resolution in FTIR is easier to obtain without sacrificing sensitivity. FTIR is especially useful for examining small samples and for taking of compounds produced in the outflow of a chromatograph. Finally, the digital form in which the data are handled in the computer allows the spectrum of a pure compound to be subtracted easily from that of a mixture to reveal the spectrum of the other components of the mixture.

Fourier transform infrared spectroscopy offers potential advantages compared with conventional dispersion infrared spectroscopy, namely:

1. higher signal-to-noise ratios for spectra obtained under conditions of equal measurement time,
2. higher accuracy in frequency for spectra taken over a wide range of frequencies

The signal-to-noise advantage is a consequence both of the concurrent measurement of the detector signal for all resolution elements of the spectrum and of the high optical throughput of the FT-IR spectrophotometer. The improvement in frequency accuracy of the FT-IR spectrophotometer is a consequence of the use of a laser which references the measurements made by the interferometer (26)

2.4.3. Sample preparation for IR:

The glass powder is finely ground and mixed with potassium bromide (in the ratio of 100:1) using pestle and mortar and grounded until the mixture becomes very fine powered so that crystallites cannot be seen. Prepare the thin disc pellet using KBR Press die. The powder is placed between two stainless still disc and transfer the sandwich onto the pistil of the hydraulic press. Move the hydraulic pump handle downward. The pistil will start to move upward until it reaches the top of the pump chamber. Then, move the pump handle upwards and pump at 6Tonnes for 6 mins. Release the pressure and remove the disks and pull apart. Remove the film, which should be homogenous and transparent in appearance. Insert into the IR sample holder and attach with scotch tape and run the spectrum.

2.5. Differential thermal analysis (dta) / thermogravimetric analysis (tg)

This Tg/DTA analyzer can simultaneously perform differential thermal analysis and thermogravimetric analysis with a single sample. Thermogravimetric analysis or thermal gravimetric analysis (TGA) is a method of thermal analysis in which changes in physical and chemical properties of materials are measured as a function of increasing temperature (with constant heating rate), or as a function of time. Thermogravimetry (TG) is a useful tool for kinetic analysis of thermal decomposition reactions. The sample is usually in the solid state and the changes that occur on heating

include melting, phase transition, sublimation, and decomposition. the analysis of the change in the mass of a sample on heating is known as thermogravimetric analysis (Tg). Tg measures mass changes in a material as a function of temperature (or time) under a controlled atmosphere. The most widely used thermal method of analysis is differential thermal analysis (DTA). In DTA, the temperature of a sample is compared with that of an inert reference material during a programmed change of temperature. the temperature should be the same until thermal event occurs, such as melting, decomposition or change in the crystal structure. If an endothermic event takes place within the sample, the temperature of the sample will lag behind that of the reference and a minimum will be observed on the curve. On the contrary, if an exothermal event takes place, then the temperature of the sample will exceed that of the reference and a maximum will be observed on the curve. The area under the endotherm or exotherm is related to the enthalpy of the thermal event. For many problems, it is advantageous to use both DTA and TG.

CHAPTER III: OBSERVATION AND DATA INTERPREPATION

3.1. Preparation of glass

Bioactive glasses with composition $\text{Na}_2\text{O}-\text{CaO}-\text{SiO}_2-\text{P}_2\text{O}_5-\text{SrO}$ were prepared by using Na_2CO_3 , CaCO_3 , SiO_2 , Na_2HPO_4 and SrCO_3 using standard melt quenching method [28,29]. All the oxides used for the preparation of glass were of analytical grade, 99.9% pure. Batch calculations were done and compounds were weighed according to the required mole percentages and then crushed to powder using a pestle and mortar and mixed to form a homogenous mixture. For trial 1, 1 gm of the mixture was ground and placed in an alumina boat and heated till a temperature of 1400-1450°C till the compound melted and a bubble free liquid was formed. A vitreous glass was formed, this was due to the presence of calcium oxide (CaO) in the melt. In the second

trial we held the melt at temperature 800 °C for 1 hour to decompose calcium oxide completely and later followed the same schedule which was used for trial 1. Using this procedure, a clear glass was obtained. First trial was carried out to find whether glass formation was possible and if so at what temperatures it was possible. Once this had been confirmed and the glass formation temperature was determined, the final samples were prepared. A heating schedule was used for glass samples and is shown in the graph in figure. After confirming the glass formation temperature, for the final sample, 10 gm of mixture was prepared and transferred into alumina crucible and heated in the furnace according to the schedule shown in the fig. (12) and fig. (13)

The melt was poured onto the steel plate. Different sizes of beads were obtained and used further for characterization. The glass melt was air quenched at 1400 °C.

The proposed composition of glass with different percentage of Cr₂O₃ were synthesized using the same schedule. The density and melting points of the compounds which were used is shown in table (3). The different proportions of the compounds used are shown in the table (4). The glass samples were characterised by XRD (Rigaku Smart-lab), FTIR (Shimadzu, Prestige 21), DTA/TGA (Shimadzu DTG -60) analysis, SEM-EDEX (JEOL EVO 18)

Table 3: Density and melting point of bioactive compounds

| Compounds | Density (g/cm ³) | Melting point (°C) |
|----------------------------------|------------------------------|--------------------|
| Na ₂ HPO ₄ | 1.7 | 250 |
| CaCO ₃ | 2.71 | 825 |
| Na ₂ CO ₃ | 2.54 | 851 |
| SrCO ₃ | 3.5 | 1494 |
| SiO ₂ | 2.65 | 1710 |
| Cr ₂ O ₃ | 5.22 | 2435 |

Table 4: Percentage table for the compounds used in the Corresponding samples

| Compounds | gm mol weight | Sample A | Sample B | Sample C | Sample D | Sample E | Sample F |
|----------------------------------|---------------|----------|----------|----------|----------|----------|----------|
| Na ₂ HPO ₄ | 141.96 | 6% | 6% | 6% | 6% | 6% | 6% |
| CaCO ₃ | 100.08 | 23% | 23% | 23% | 23% | 23% | 23% |
| Na ₂ CO ₃ | 105.98 | 23% | 23% | 23% | 23% | 23% | 23% |
| SrCO ₃ | 147.63 | 3% | 3% | 3% | 3% | 3% | 3% |
| SiO ₂ | 60.08 | 45% | 44.95% | 44.9% | 44.7% | 44.5% | 44% |
| Cr ₂ O ₃ | 151.99 | 0% | 0.05% | 0.1% | 0.3% | 0.5% | 1% |

Formula:

$$\text{Corrected weight} = \frac{\text{gram mole} \times \text{desired percentage of the compound}}{100}$$

$$\text{Desired weight of the sample} = \frac{\text{Corrected weight} \times \text{gramage of compound}}{\text{Sum of the corrected weight}}$$

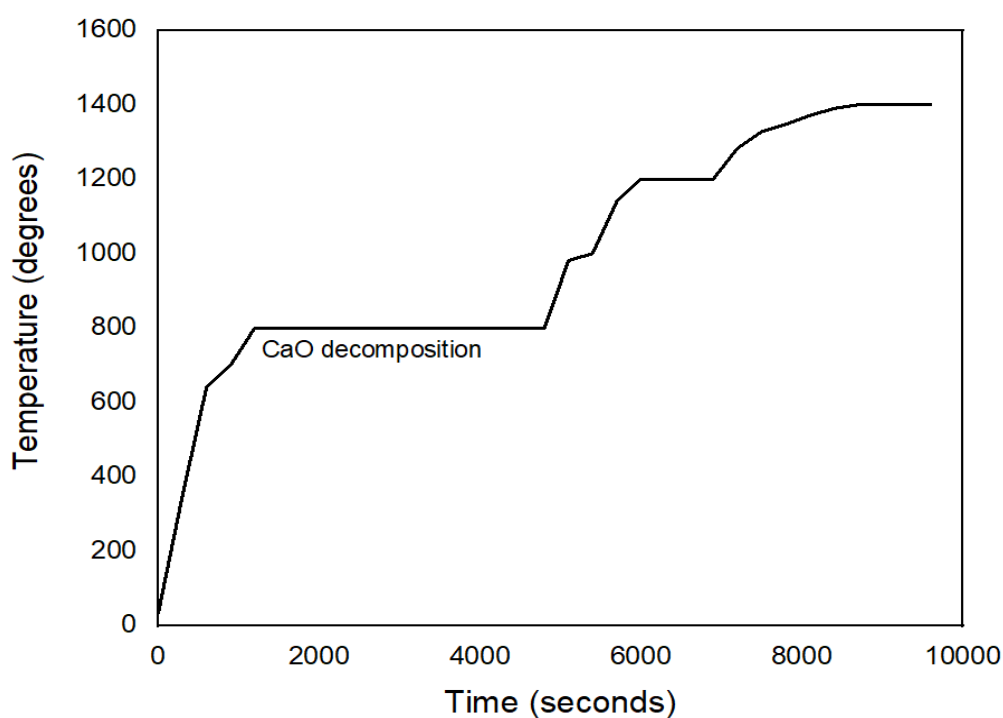


Figure 12: Temperature and time relation graph for Sample A (0% Cr₂O₃)

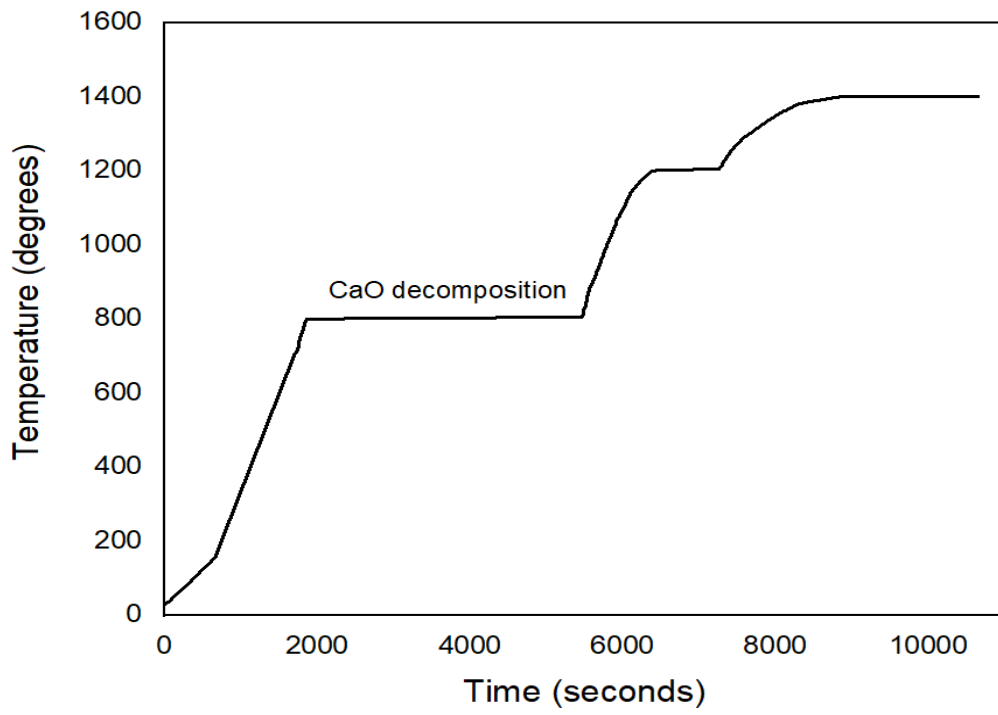


Figure 13: Temperature and time relation graph for Sample B (0.05% Cr₂O₃)



Figure 14: Preparation of Glass samples



Figure 15: Preparation of glass samples



Figure 16: Prepared Glass samples



Figure 17: Glass beads of various percentages of Cr_2O_3

3.3. Characterisation, Data Interpretation and results

3.3.1. Density measurements on glass Sample beads

Density measurements were carried out in two steps. One, we found the weight of the glass beads using weighing machine, precautions were taken that glass beads without air bubbles formed in it were only used. In step two, the volume of the corresponding glass beads was found using Archimedes water displacement method. Density was calculated using formula

$$density = \frac{mass}{volume} \quad (3)$$

The density values obtained for different composition of glass are given in the table (5)

Table 5: Density of the glass Samples

| Sr. No | Glass sample | Density gm/cm ³ |
|--------|---------------------|----------------------------|
| 1 | Sample A – Cr 0% | 2.7537 |
| 2 | Sample B – Cr 0.05% | 2.7702 |
| 3 | Sample C – Cr 0.1% | 2.7985 |
| 4 | Sample D – Cr 0.3% | 2.8445 |
| 5 | Sample E – Cr 0.5% | 2.8307 |
| 6 | Sample F – Cr 1% | 2.8504 |

Table (5) shows the densities of glass composition with varying percentage of Cr₂O₃ (glass A - Cr - 0%, Glass B Cr - 0.05 %, glass C - Cr-0.1%, glass D - Cr-0.3%, glass E – Cr - 0.5% , glass F – Cr - 1%). As observed from the table the densities increase with increase in chromium content. The densities vary from 2.7537 to 2.8504 gm.cm⁻³. This increase may be attributed to the fact that in the glasses the Cr₂O₃ is partially replaced by SiO₂. In this case the density of SiO₂ which is around 2.63 is replaced by heavier element Cr₂O₃ of density 5.22 gm.cm⁻³.

3.3.2. X Ray Diffraction

The glass beads were ground into powder which was used to carry out XRD. X-ray diffraction measurements on the glass samples were carried out using Rigaku Smart-lab diffractometer with incident $\text{CuK}\alpha$ (1.5406 Å) radiation source at 40 to 50kV at 40 mA. The data was collected in the angular range from 10° to 100° in a step size of 0.01° and measuring speed was set to 5° per min. X-ray diffraction is used to identify the crystalline or amorphous nature of the synthesized samples. The XRD spectrum of all the samples of glasses obtained are shown graphically in Figure (18 – 24).

The XRD pattern of glass with and without Cr_2O_3 shows no Bragg's peak, but only a broad diffuse hump around low angle region at around 31° for all the samples. Clearly indicating amorphous nature of the glass samples. X-ray diffraction pattern on these glasses confirmed their glassy nature which is structurally similar.

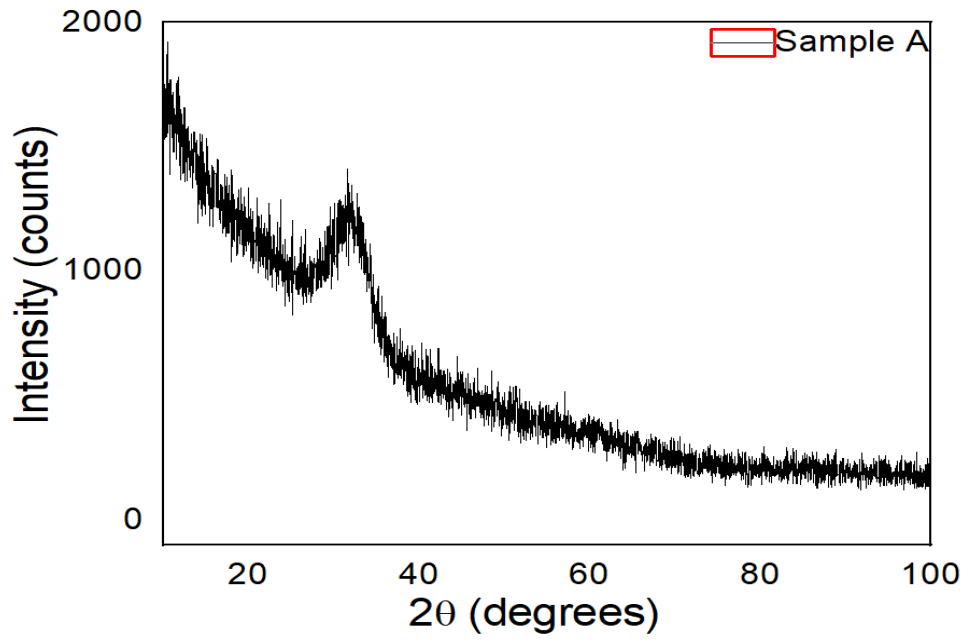


Figure 18: X-ray spectrum of sample A

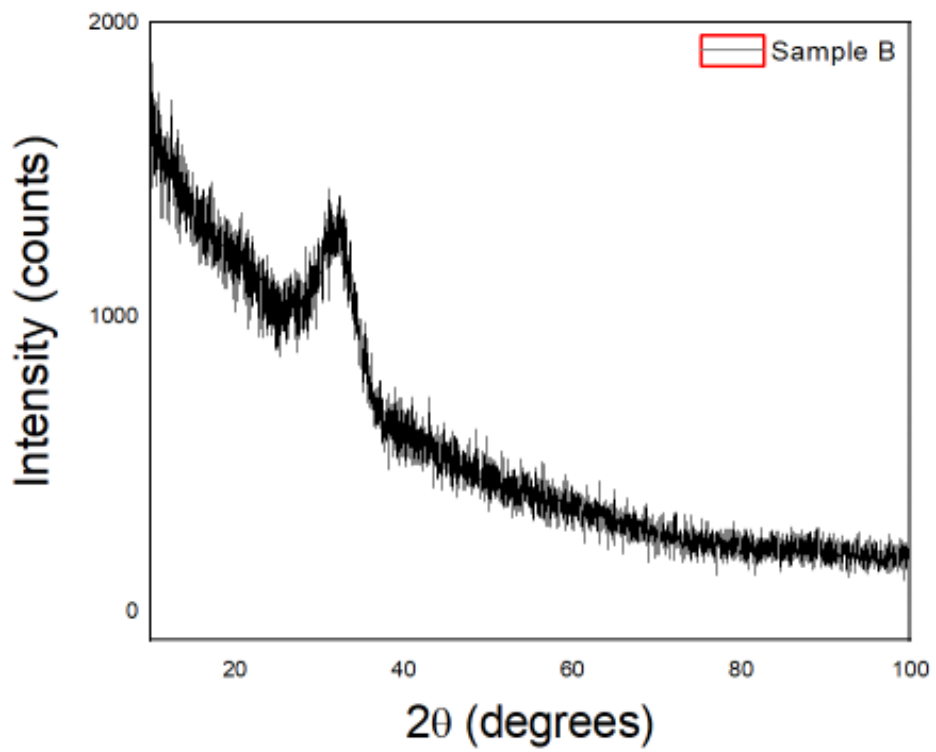


Figure 19: X-ray spectrum of sample B

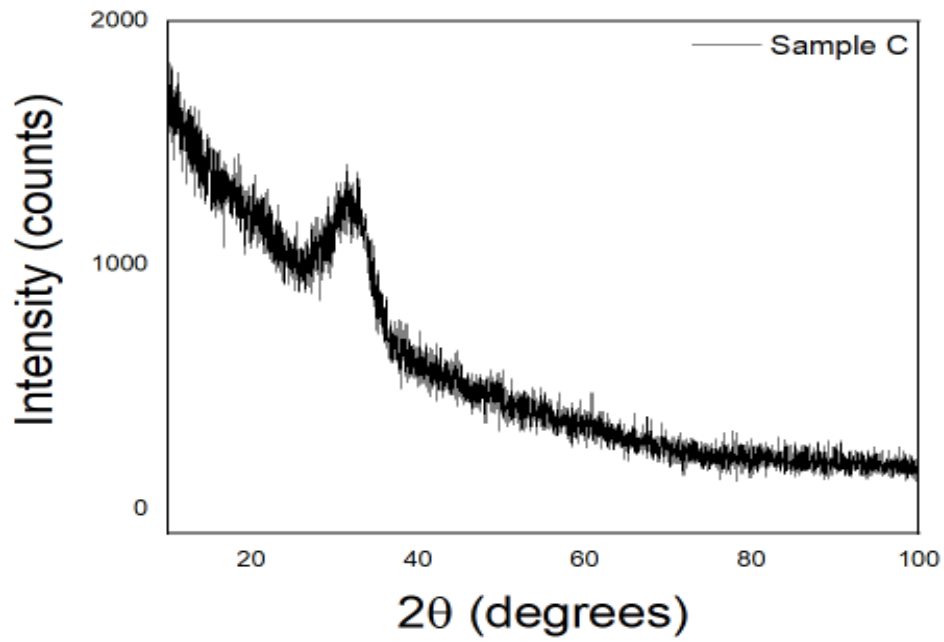


Figure 20: X-ray spectrum of sample C

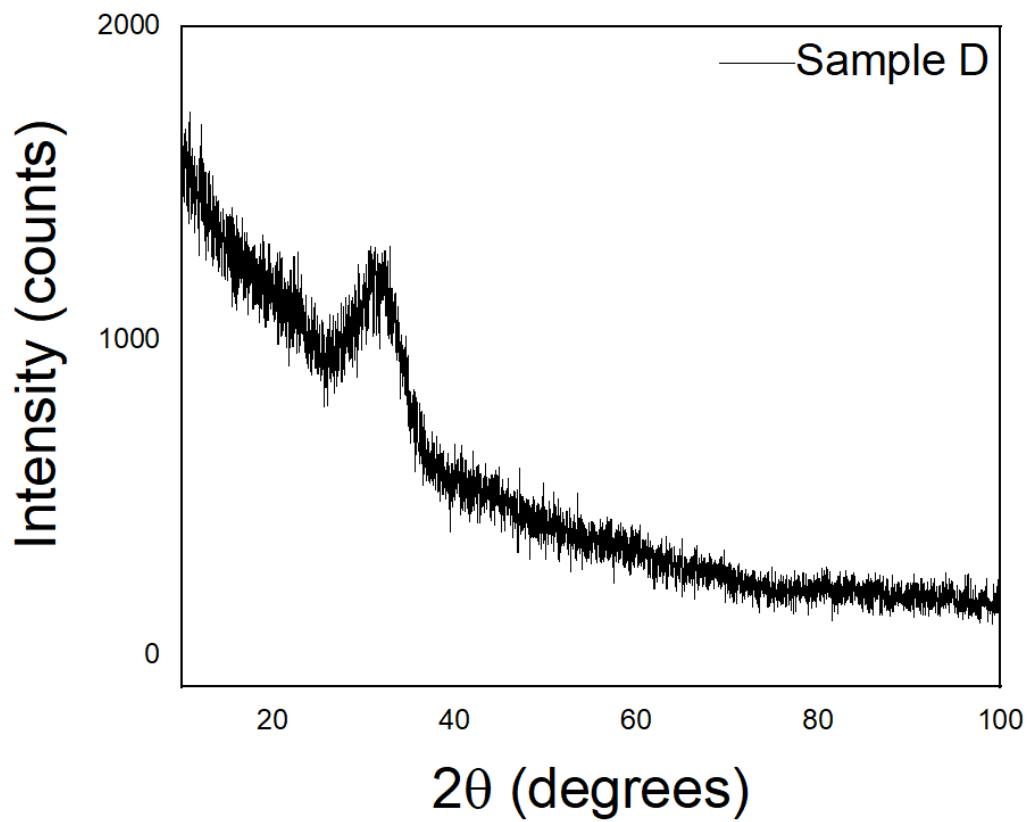


Figure 21: X-ray spectrum of sample D

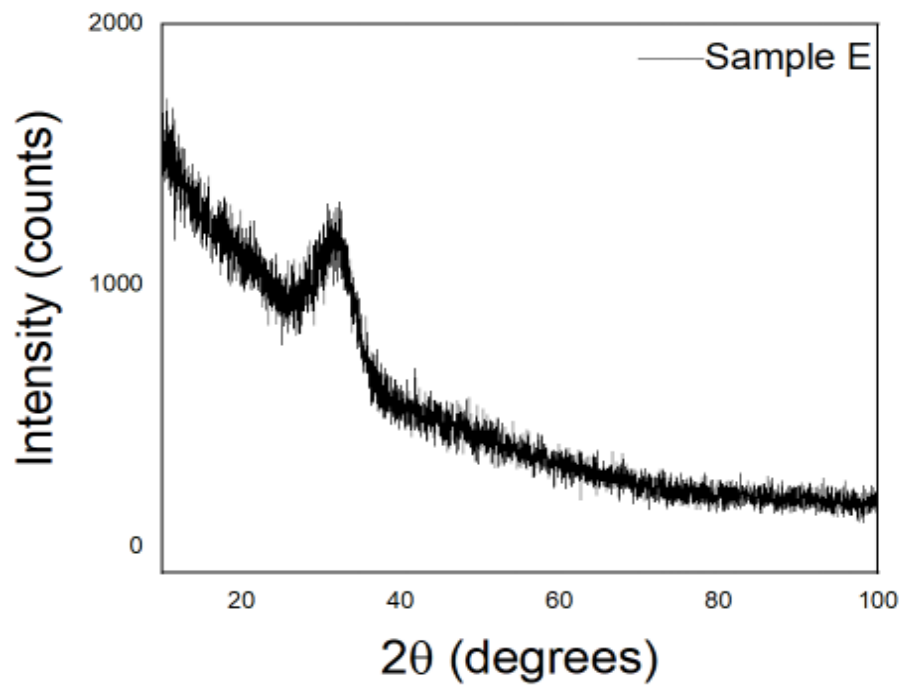


Figure 22: X-ray spectrum of sample E

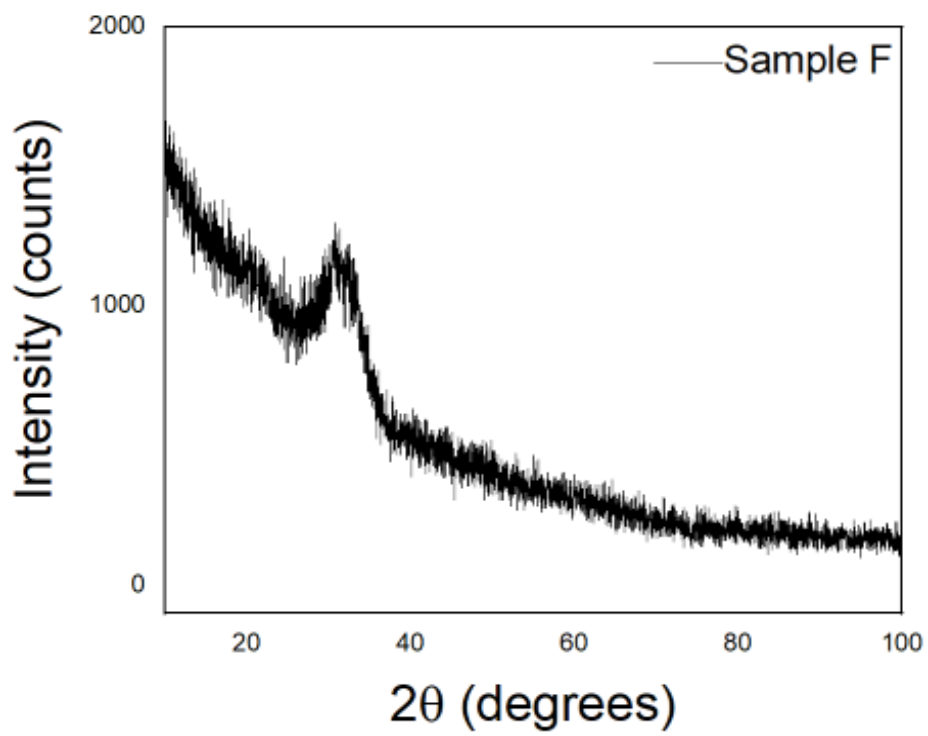


Figure 23: X-ray spectrum of sample F

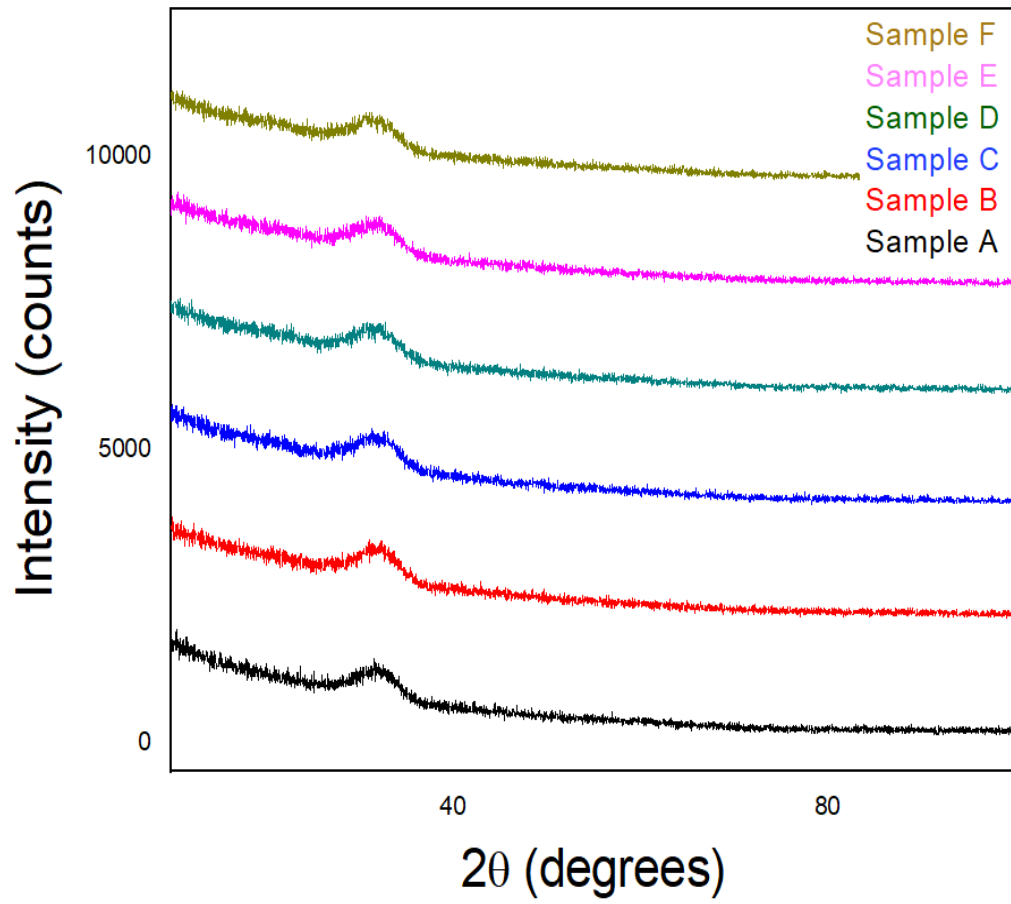


Figure 24: X-ray spectrum of all samples clubbed together

3.3.3. IR spectroscopy

IR studies were carried out to determine different types of bonds present in the glass sample. Infra-red absorption spectra for all six samples were obtained on a Shimadzu 8900 Infra-red Spectrometer in the wave number range 400 cm^{-1} to 4000 cm^{-1} . Samples were mixed with KBr in the ration 1:100 and the pellets were prepared for the experiment. OH and CO_2 in the environment around the sample is shown as small features between 1500 cm^{-1} and 2000 cm^{-1} in all the samples. Si-O-Si symmetric bending is observed at around 490 cm^{-1} and 896 cm^{-1} corresponding to symmetric stretching is observed in all the glass samples confirming the host matrix of the bio glass to be silica (as expected). The glass sample are a combination of glass former SiO_2 and P_2O_5 , intermediate oxide Na_2O and modifier SrO. The infrared spectra of glass samples studied exhibited different bands due to vibration of silicate, phosphate structural units are shown in table (7).

The band at 1047 cm^{-1} can be attributed to Si-O-Si stretching. The small band at 1467 cm^{-1} is attributed to C-O vibrational mode. The phosphate group peaks are observed at 678 , 654 and 571 cm^{-1} . P-O bending is observed at 654 cm^{-1} in all the glasses which is characteristic of calcium phosphate. The increase in chromium content does not show major changes in the glass structure. As the concentration of Cr_2O_3 is increased upto 1%, a significant increase in the intensity of asymmetrical vibrational band is observed. The table shows all the peaks observed in the IR spectrum of the glass sample.

Table 6: Peaks of the IR spectrum

| Wavenumber cm ⁻¹ | Functional groups |
|-----------------------------|--------------------------|
| 400-500 | Si-O-Si (bend) |
| 500-560 | P-O (bend) (crystalline) |
| 560-600 | P-O (bend)(Amorphous) |
| 720-840 | Si-O-Si (Tetrahedral) |
| 860-940 | Si-O (Stretch) |
| 1000-1100 | Si-O-Si (Stretch) |
| 1100-1200 | P-O (Stretch) |
| 1400-1530 | C-O (Stretch) |
| 1600-1900 | C=O (Stretch) |
| 3000-3700 | O-H (Stretch) |

Table 7: IR spectrum data showing peaks for all the glass samples

| Sample | Peak 1 | Peak 2 | Peak 3 | Peak 4 | Peak 5 | Peak 6 | Peak 7 | Peak 8 | Peak 7 | Peak 8 |
|----------|-----------|-----------|-----------|-----------|-----------|-----------|-----------|-----------|-----------|-----------|
| Sample A | 1654 | 1487 | 1423 | 1047 | 977 | 896 | 678 | 654 | 571 | 490 |
| Sample B | 1681 | 1490 | 1411 | 981 | 914 | 732 | - | 659 | 573 | 499 |
| Sample C | 1649 | 1487 | 1423 | 1056 | 972 | 902 | 674 | 650 | 528 | 487 |
| Sample D | - | 1484 | 1411 | 1053 | 977 | 905 | 681 | 652 | 573 | 496 |
| Sample E | 1657 | 1487 | 1417 | 1065 | 983 | 907 | 687 | 654 | 568 | 490 |
| Sample F | 1640 | 1487 | 1417 | 1044 | 983 | 904 | 678 | 654 | 571 | 490 |

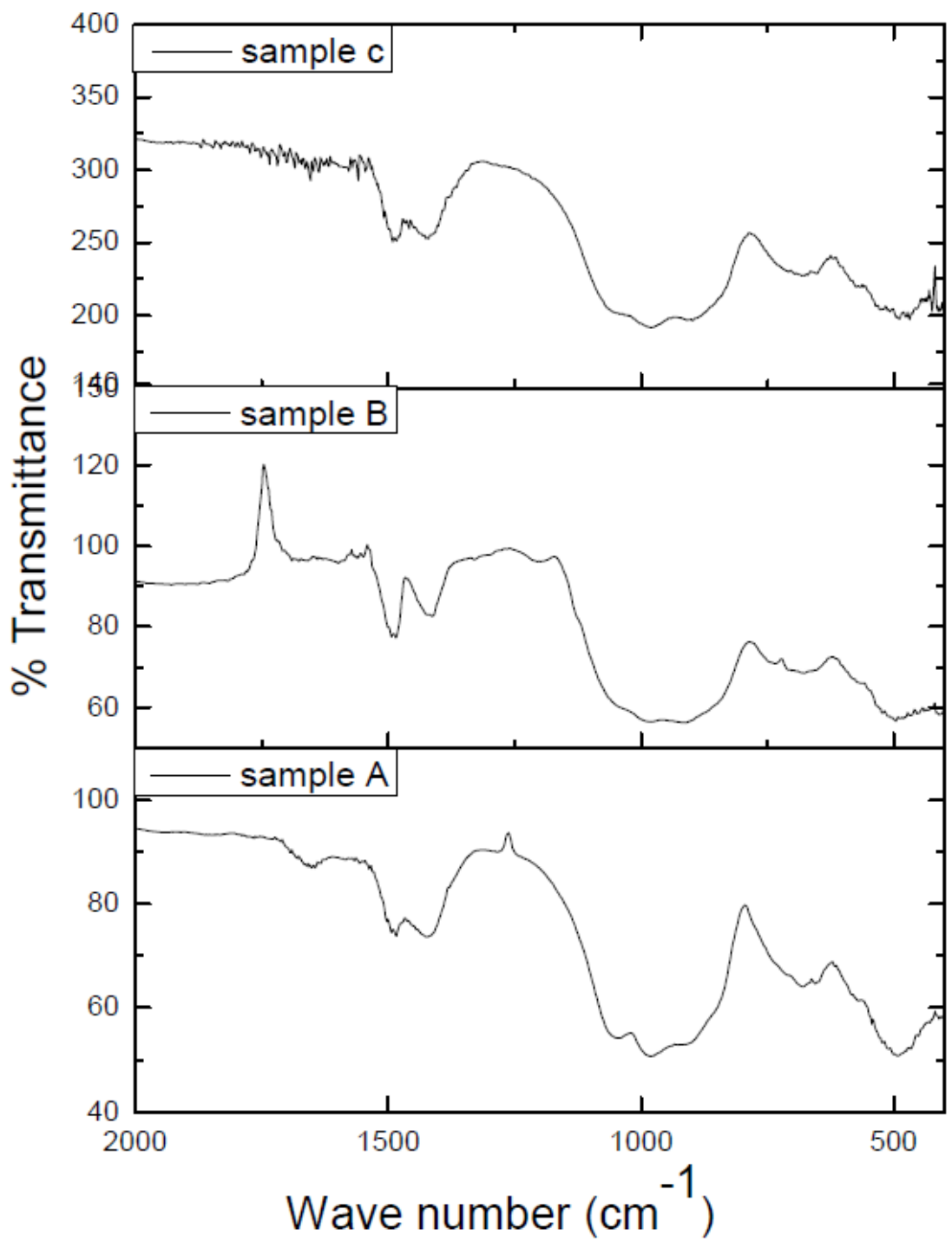


Figure 25: IR spectrum of sample A, B & C

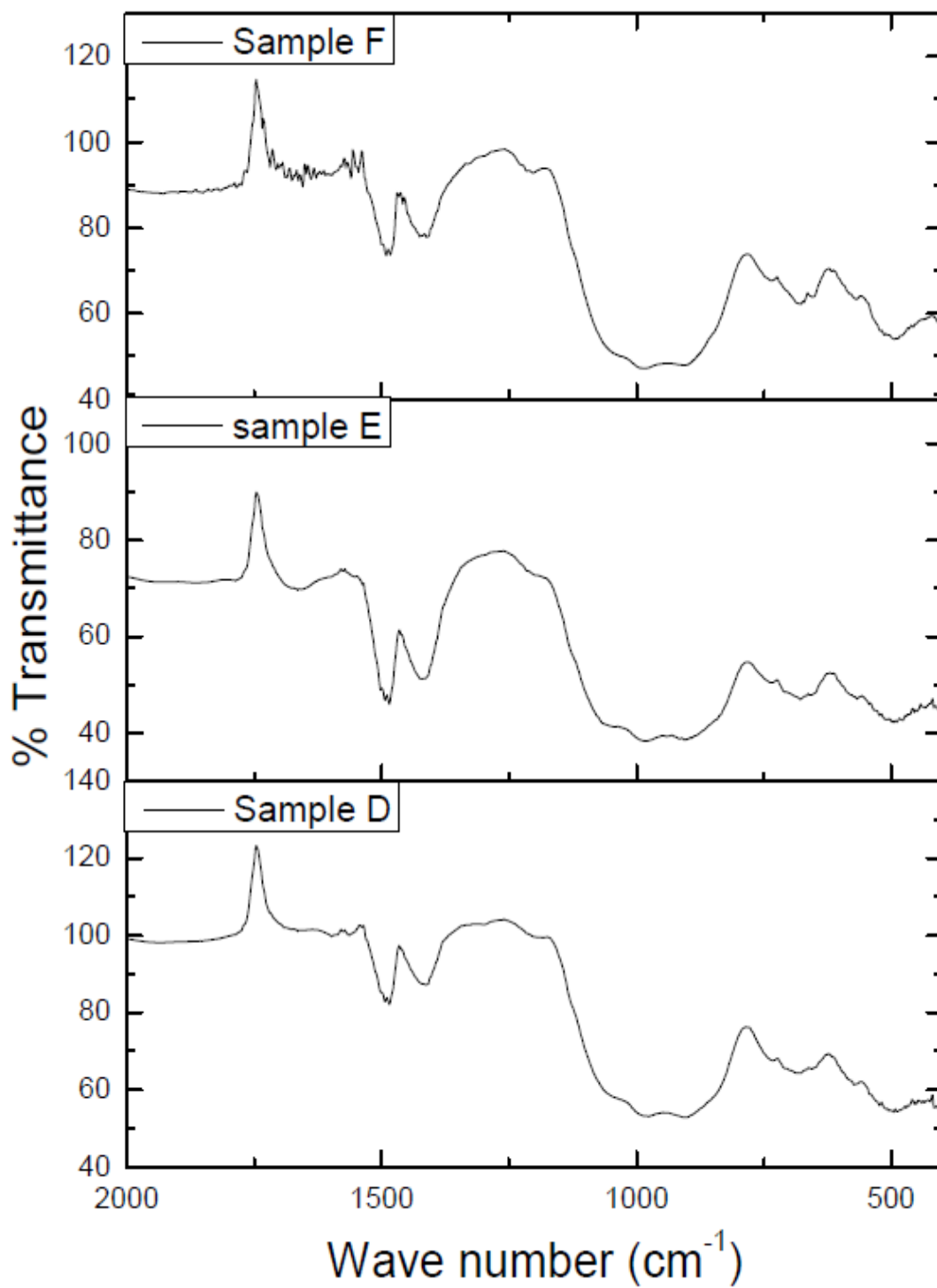
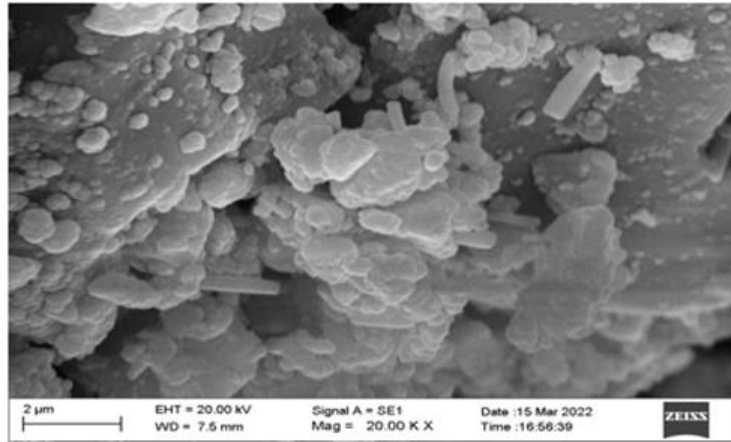


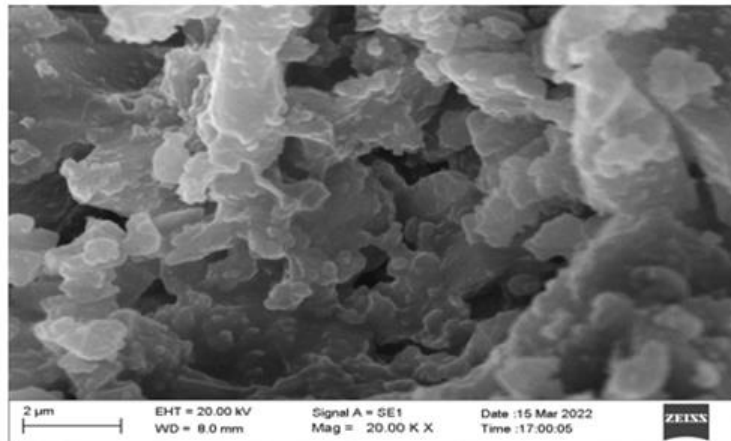
Figure 26: IR spectrum of sample D, E & F

3.3.4. SEM EDS

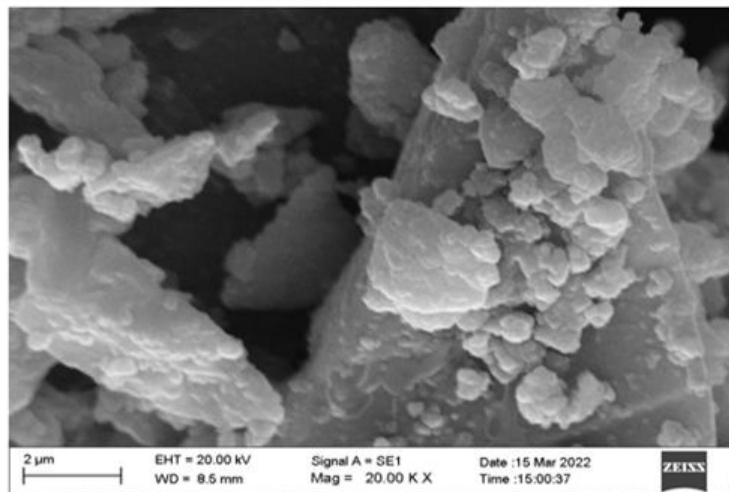
The Scanning electron microscope (SEM) micrographs were obtained at a magnification of 20,000 using the Joel SEM (EVO18). The micrographs of the untreated (with SBF) glass samples are shown in figure (27 & 28). It shows a heterogeneous surface. The surface shows the dense polycrystalline fine texture of the powder which appears covered by flakes of smaller particles. The EDS data is shown in the figure (29 & 30) and the elemental composition in each sample is shown in table (8).



Sample A

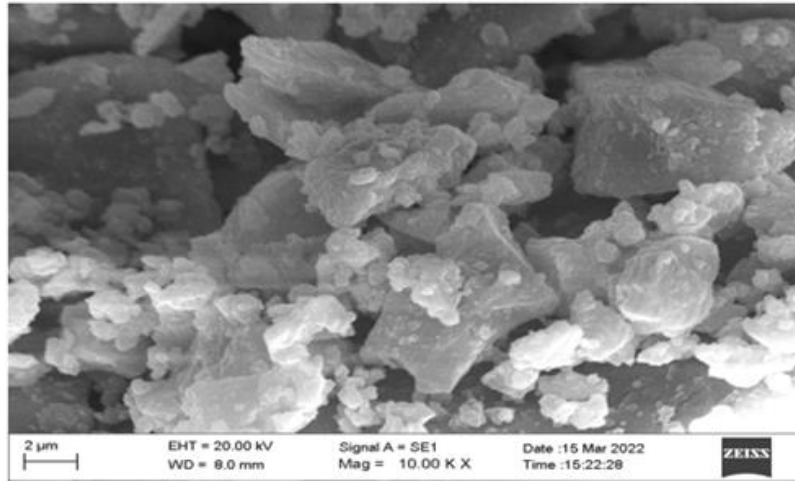


Sample B

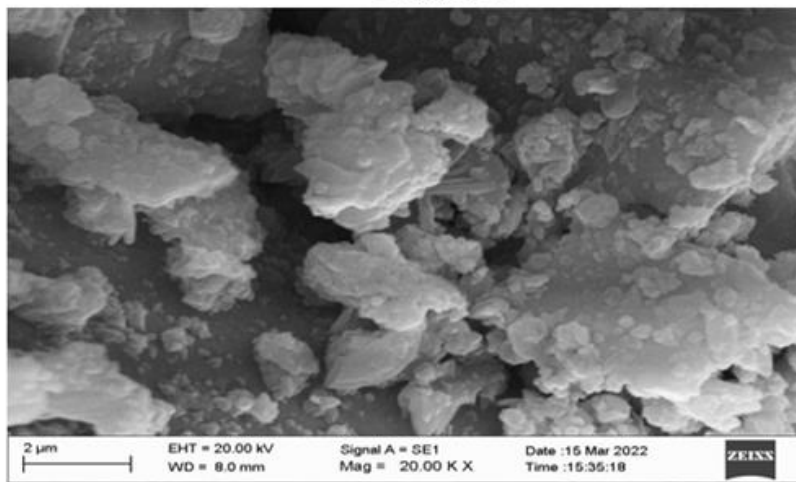


Sample C

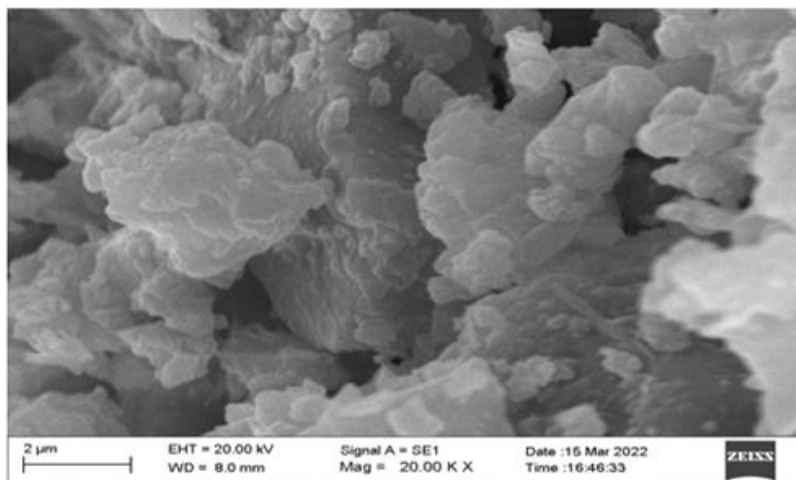
Figure 27: SEM images of sample A, B & C



Sample D



Sample E



Sample F

Figure 28: SEM images of sample D, E & F

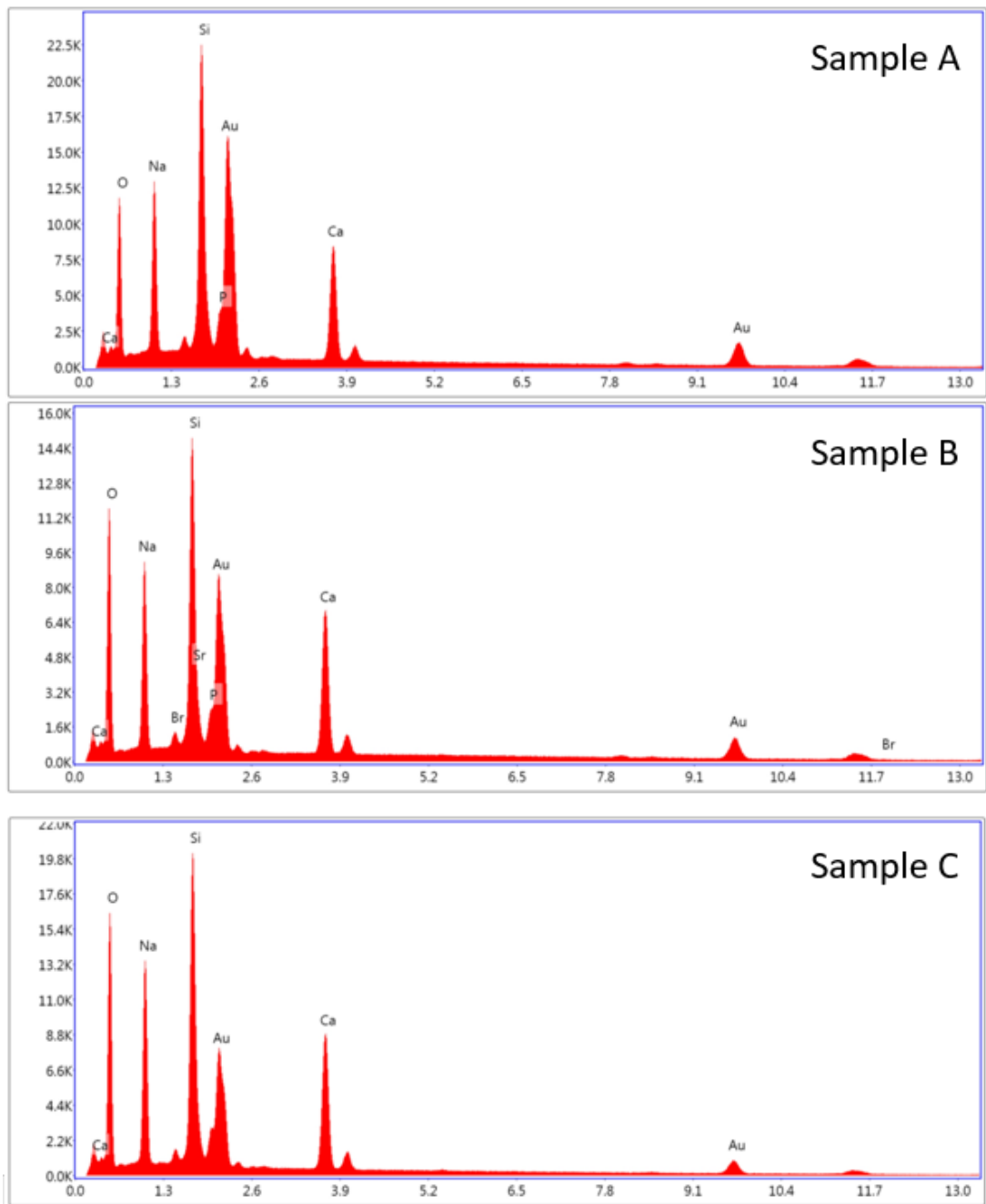


Figure 29: Eds data of sample A B & C

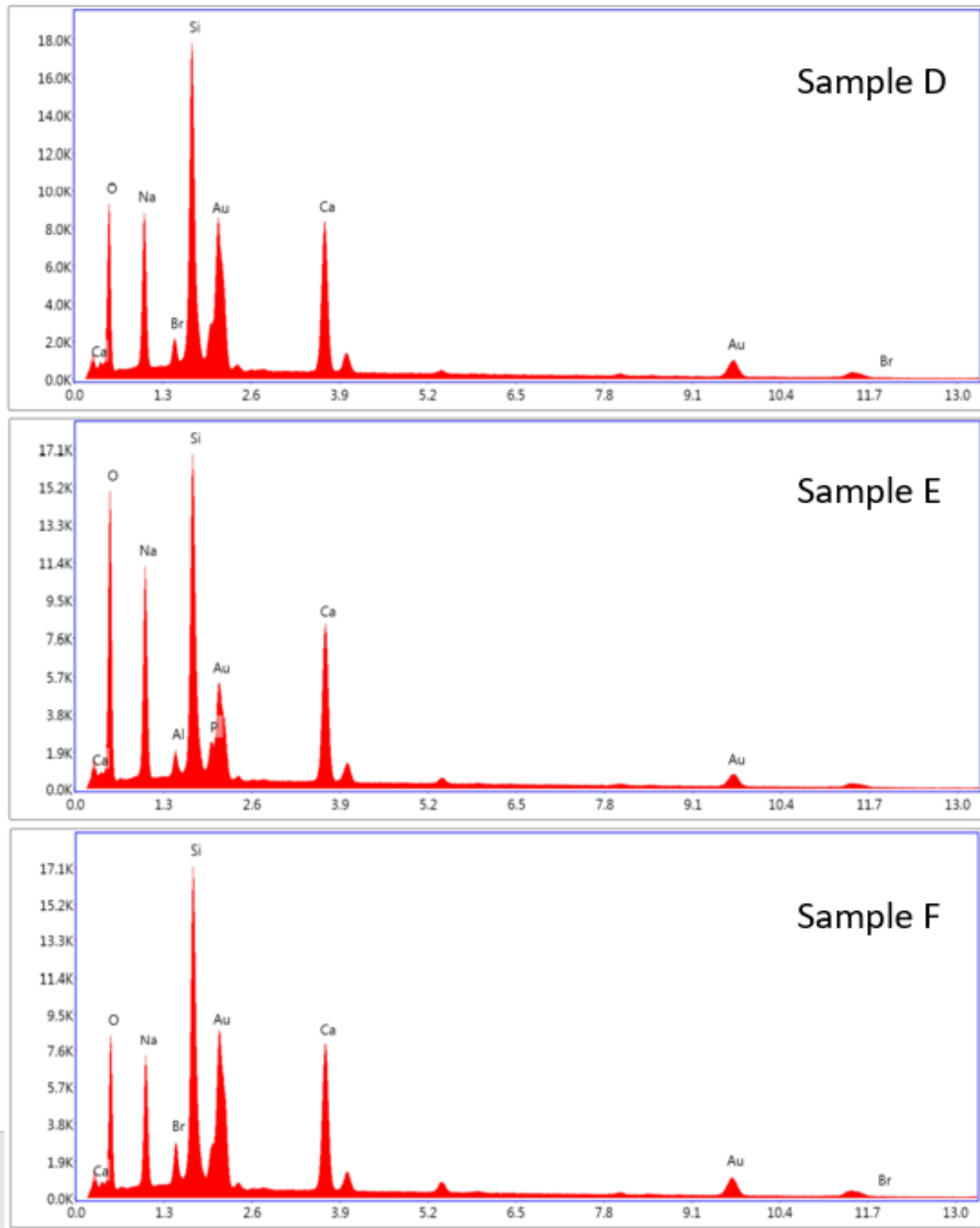


Figure 30: EDS data of sample A, E & F

Table 9: Eds data showing various weight percentages of the elements

| ELEMENTS | Sample A | Sample B | Sample C | Sample D | Sample E | Sample F |
|----------|----------|----------|----------|----------|----------|----------|
| OK% | 17.48 | 19.50 | 33.72 | 24.43 | 31.68 | 24.69 |
| NaK% | 12.85 | 12.60 | 16.97 | 15.42 | 14.62 | 8.97 |
| AlK% | | | | 1.70 | 1.02 | 2.04 |
| SiK% | 13.59 | 11.31 | 18.45 | 14.35 | 17.63 | 12.23 |
| PK% | 2.11 | 2.14 | 2.53 | 3.02 | 2.51 | 1.78 |
| CaK% | 11.22 | 10.84 | 15.83 | 12.62 | 18.47 | 10.54 |
| CrK% | - | - | - | - | - | 1.15 |
| AuL% | 42.75 | 41.99 | 12.5 | 27.26 | 9.44 | 38.60 |
| SrL% | - | 2.87 | - | 4.22 | 4.21 | - |

3.3.5. Thermogravimetric analysis

Thermogravimetric analysis was carried out using a NETZSCH STA 409 PC TG-DTA instrument. Thermo-gravimetric measurements in which the glass powder was heated at a constant rate at room temperature in air while recording its change in mass.

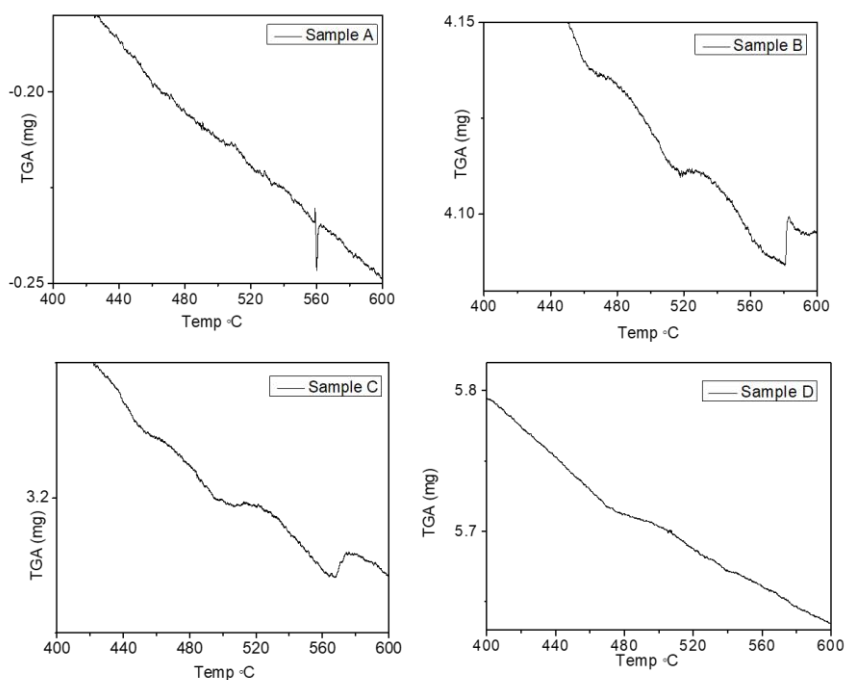


Figure 31: TGA data of the glass sample A, B, C & D

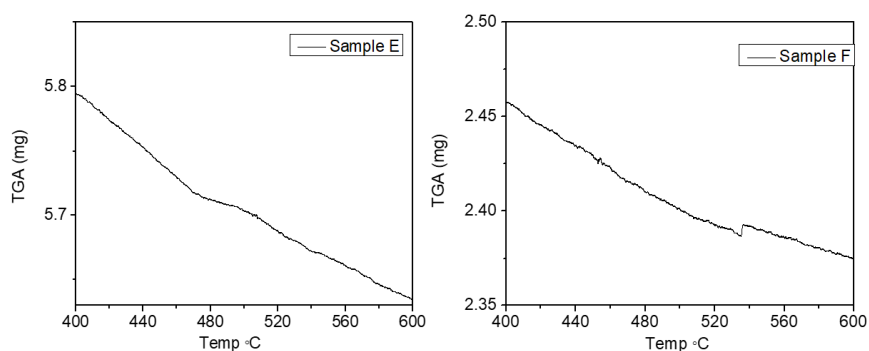


Figure 32: Graphs of TGA for sample E & F

From TGA data the glass transition temperature obtained for the samples is given in table (10). The glass temperature is found to be decreased with increase in chromium content in the composition.

Table 10: Tg temperature of all the glass samples

| Sr. No | Glass sample | T _g °C |
|--------|---------------------|-------------------|
| 1 | Sample A – Cr 0% | 560 |
| 2 | Sample B – Cr 0.05% | 580 |
| 3 | Sample C – Cr 0.1% | 567 |
| 4 | Sample D – Cr 0.3% | 539 |
| 5 | Sample E – Cr 0.5% | 539 |
| 6 | Sample F – Cr 1% | 535 |

3.3. In vitro study of Bioactive glass

3.3.1. Preparation of SBF solution and loading in the glass compacts

Simulated body fluid was prepared according to the Kokubo et al[21]. Chemicals were weighed as given in the table and mixed in the beaker one by one. The maintain the Ph at 7.4 more 10 ml of 1 N HCl was added in the beaker. The prepared SBF was preserved in refrigerator.

Table 11: Weight of compounds used for SBF solution preparation

| Order | Reagent | Amount |
|---|---|---------|
| 1 | NaCl | 7.996 g |
| 2 | NaHCO ₃ | 0.350 g |
| 3 | KCl | 0.224 g |
| 4 | K ₂ HPO ₄ · 3H ₂ O | 0.228 g |
| 5 | MgCl ₂ · 6H ₂ O | 0.305 g |
| 6 | 1M-HCl | 40 mL |
| (About 90 % of total amount of HCl to be added) | | |
| 7 | CaCl ₂ | 0.278 g |
| 8 | Na ₂ SO ₄ | 0.071 g |
| 9 | (CH ₂ OH) ₃ CNH ₂ | 6.057 g |

To check the formation of hydroxyapatite layer on the glass powder, the glass beads were crushed to fine powder and pallets of diameter 13 mm and thickness 1 mm were prepared in KBr die at 6 Ton pressure. The ion content of human blood is same as that of SBF solution formed.

Table 12: Ion concentration(mM) of SBF and human blood plasma

| Ion | Simulate Body Fluid | Blood plasma |
|--------------------------------|---------------------|--------------|
| Na ⁺ | 142.0 | 142.0 |
| K ⁺ | 5.0 | 5.0 |
| Mg ²⁺ | 1.5 | 1.5 |
| Ca ²⁺ | 2.5 | 2.5 |
| Cl ⁻ | 148.8 | 103.0 |
| HCO ₃ ⁻ | 4.2 | 27.0 |
| HPO ₄ ²⁻ | 1.0 | 1.0 |
| SO ₄ ²⁻ | 0.5 | 0.5 |

The freshly prepared Simulated body fluid (SBF) was infused in the pallets and kept at room temperature. The surface morphology and microstructure of Bioactive glass tablets after immersing in SBF were characterised by SEM and XRD.

3.3.2. XRD on Bio glass after immersion of glass tablets in SBF

The immersion of sample in simulated body fluid was kept for 21 days. Xray data was obtained after 21 days. A crystalline phase is superimposed on the amorphous phase as indicated in the graphs below. The amorphous phase before incubation showed some small peaks indicating the crystallisation of the material. After 21 days incubation sharp peaks were seen corresponding to apatite layer and calcite.

The XRD data, in figure (33 – 40) shows the composition of the calcium phosphate crystal growth on the glass surfaces. The obtained results confirmed bioactivity of the bioactive glass in the study.

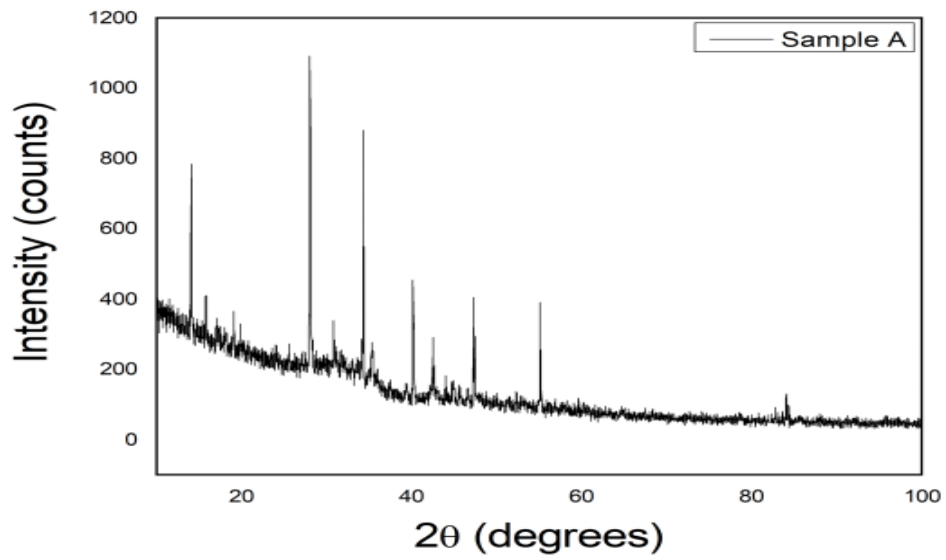


Figure 33: X-ray spectrum of sample A after incubation in SBF

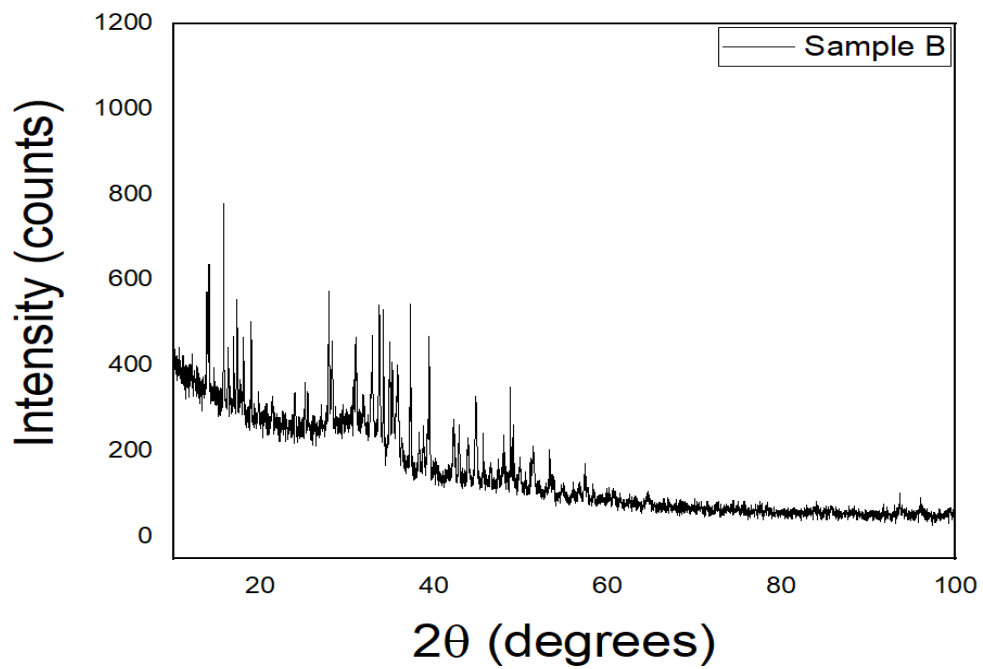


Figure 34: X-ray spectrum of sample B after incubation in SBF

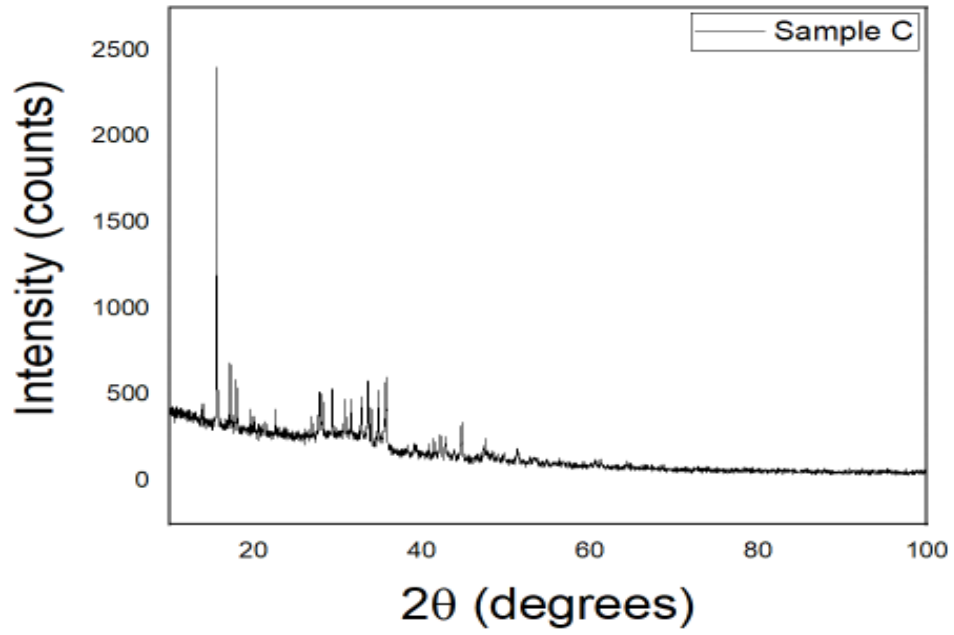


Figure 35: X-ray spectrum of sample C after incubation in SBF

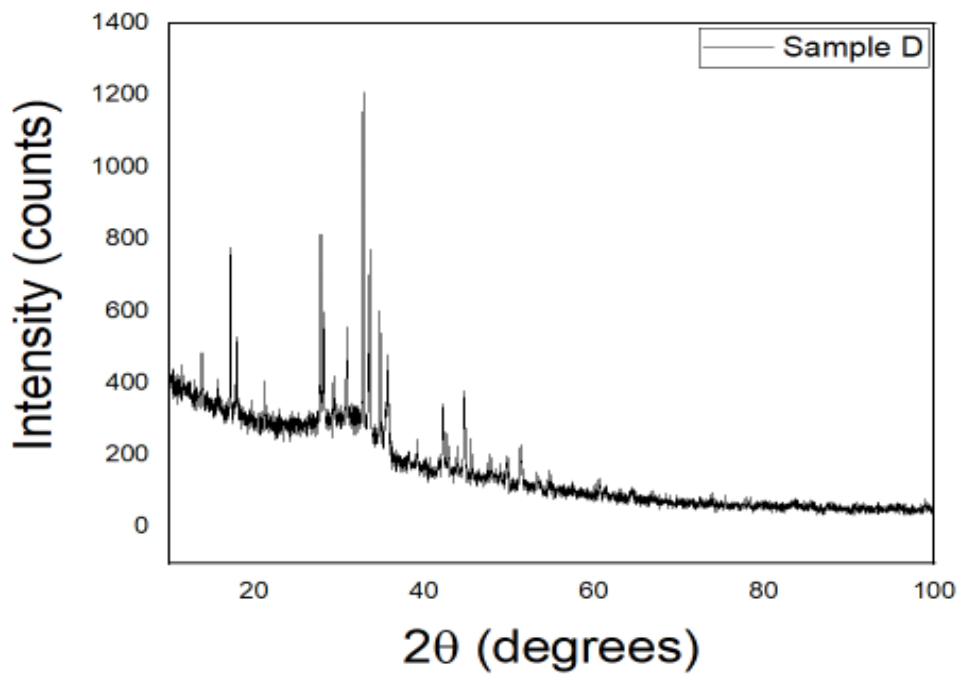


Figure36: X-ray spectrum of sample D after incubation in SBF

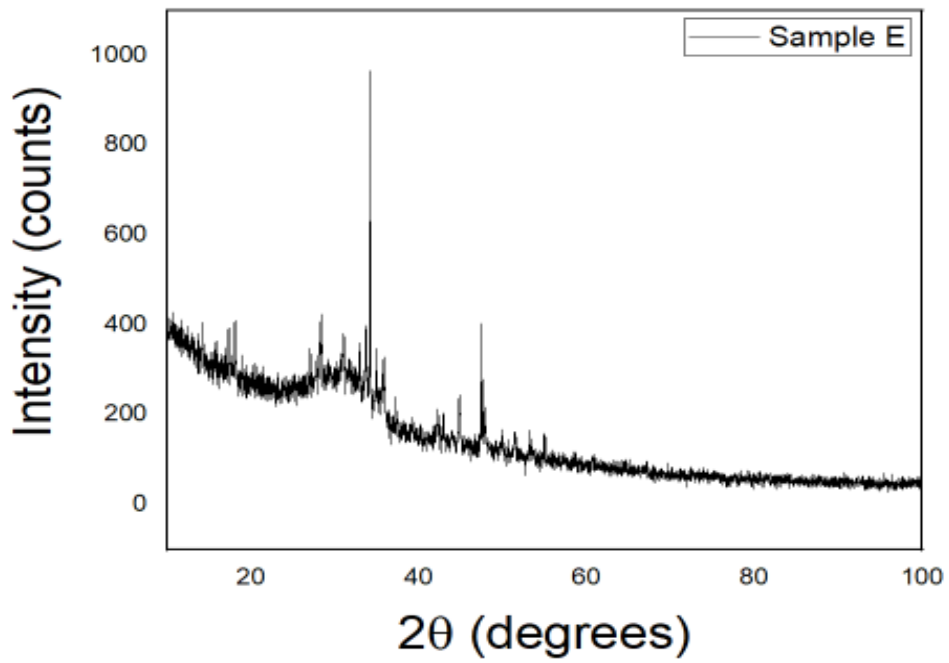


Figure 37: X-ray spectrum of sample E after incubation in SBF

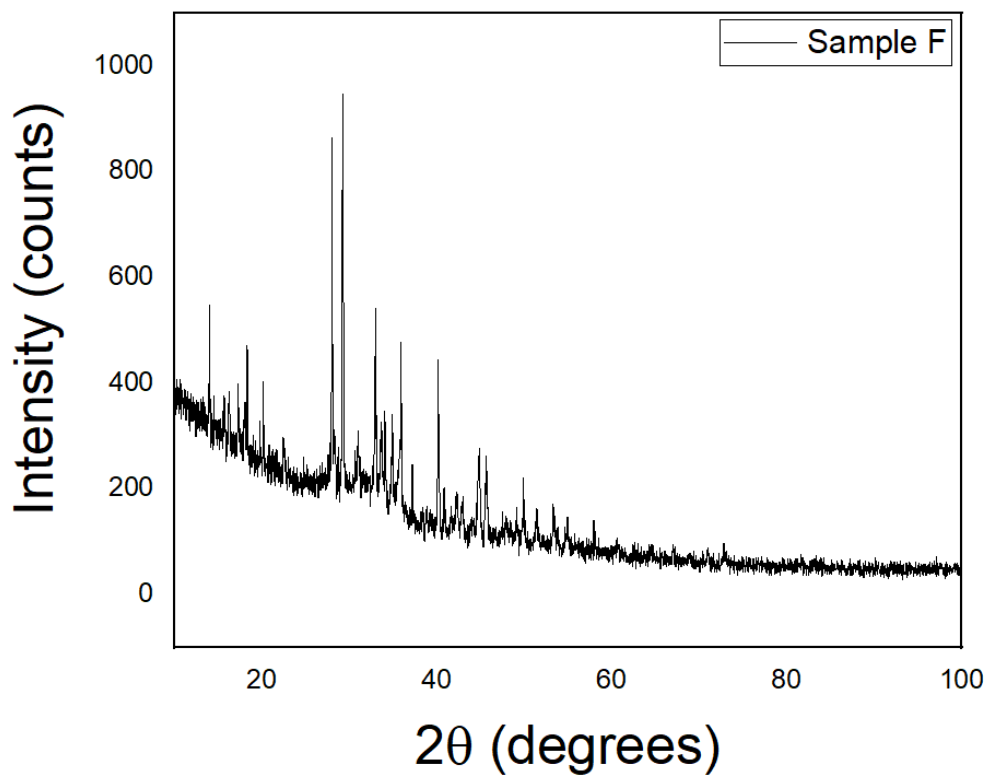


Figure 38: X-ray spectrum of sample F after incubation in SBF

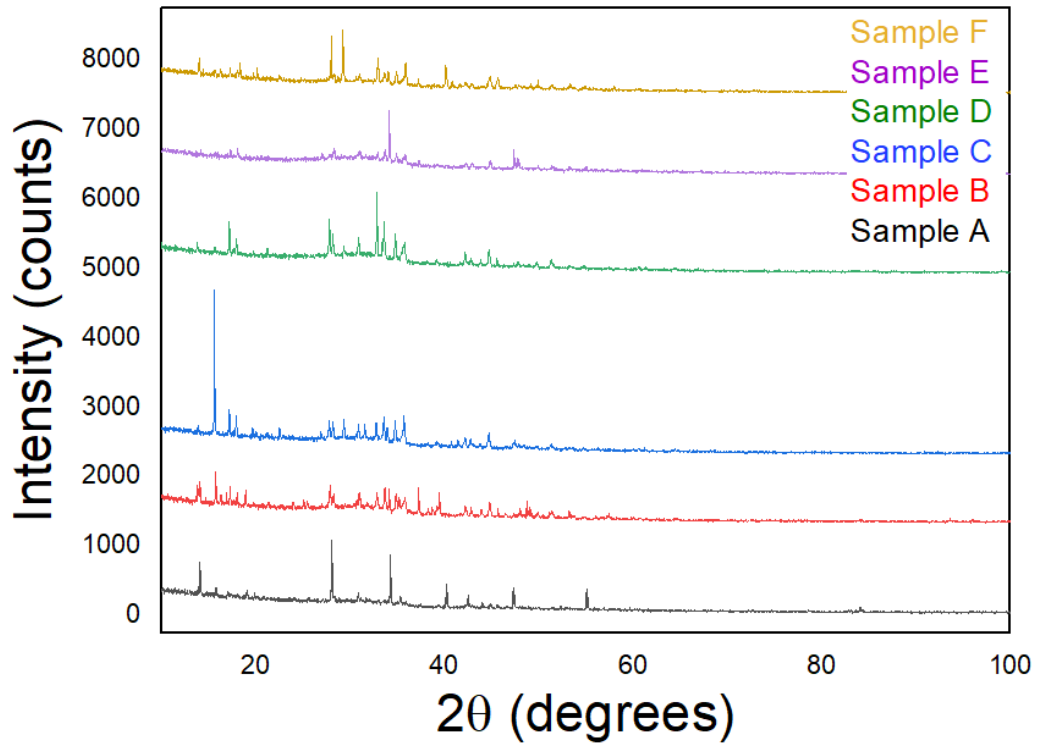
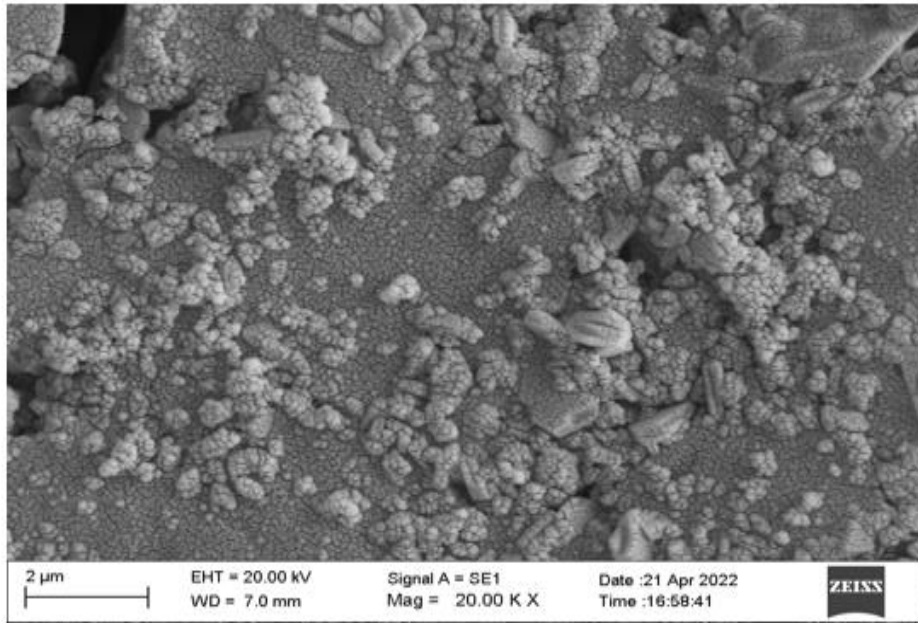


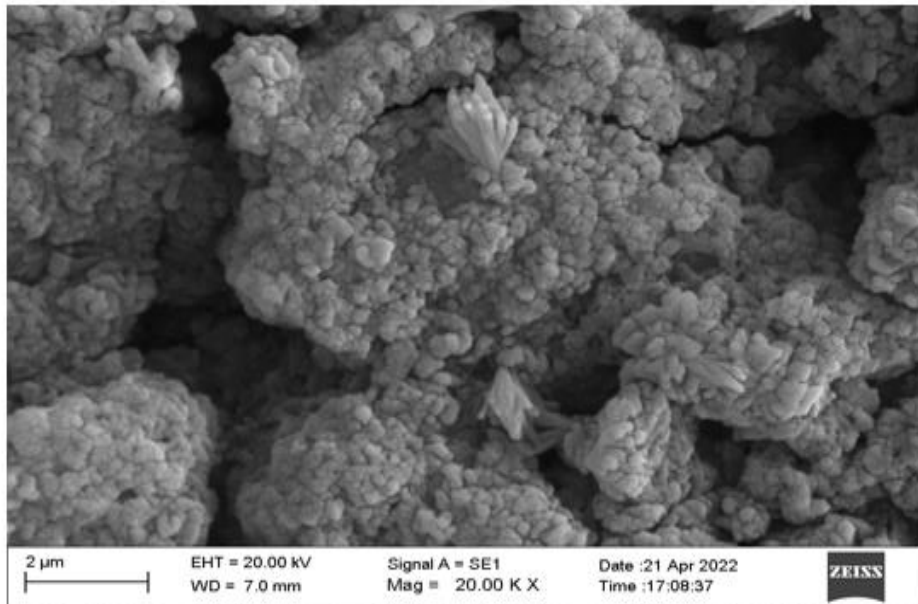
Figure 40: X-ray spectrum of all the samples after incubation in SBF

3.3.3. SEM and EDS after immersion of glass tablets in SBF solution

The micrographs of SBF treated glass powder are shown in figure (41- 43). The surface appears to be covered by a small precipitates of apatite layer. The 30 days of SBF immersion a layer of spherical particles fully covering the materials surface can be observed. EDS study shows the absence of Si in the layer composition. Micrographs show evolution of apatite deposition on the surface of the powder. It shows on the glass surface some few scarcely distributed spherical beads which can be attributed to the deposition of calcium phosphate. Size of the spheres is found to slightly in samples containing chromium.

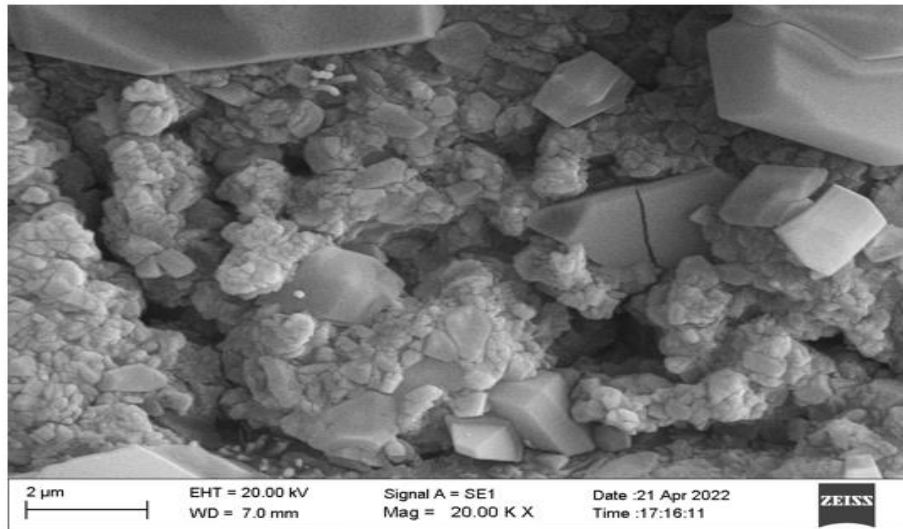


Sample A



Sample C

Figure 41: SEM images of sample A & C after incubation in SBF



Sample F

Figure 42: SEM images of sample F after incubation in SBF

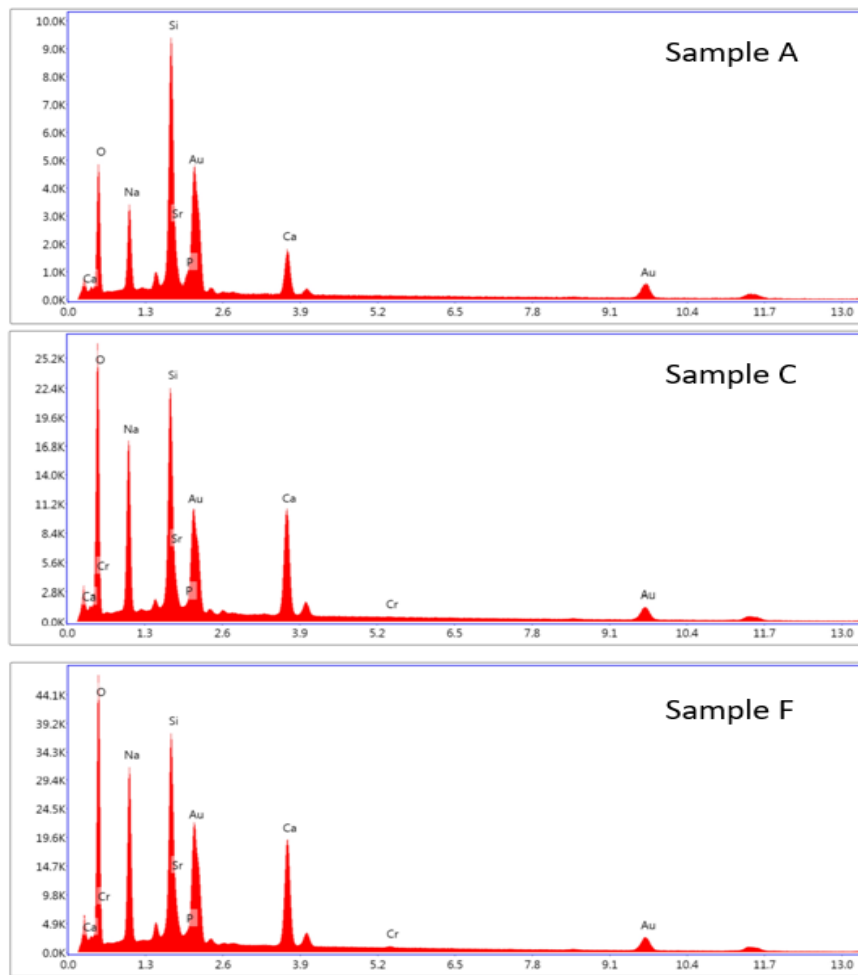


Figure 43: Eds data of sample A, C &F after incubation in SBF

Table 13: Elemental composition before and after loading SBF in Glass tablets

| ELEMENTS | Sample A | Sample A with SBF | Sample C | Sample C with SBF | Sample F | Sample F with SBF |
|----------|----------|----------------------|----------|----------------------|----------|----------------------|
| OK% | 17.48 | 18.14 | 33.72 | 26.21 | 24.69 | 20.96 |
| NaK% | 12.85 | 7.18 | 16.97 | 11.89 | 8.97 | 10.51 |
| AlK% | - | - | - | - | 2.04 | - |
| SiK% | 13.59 | 17.43 | 18.45 | 19.81 | 12.23 | 11.05 |
| PK% | 2.11 | 0.84 | 2.53 | 0.39 | 1.78 | 0.84 |
| CaK% | 11.22 | 5.77 | 15.83 | 7.49 | 10.54 | 10.64 |
| CrK% | - | - | - | 0.07 | 1.15 | 0.56 |
| AuL% | 42.75 | 46.29 | 12.5 | 29.39 | 38.60 | 30.55 |
| SrL% | - | 4.36 | - | 4.77 | - | 5.90 |

CHAPTER IV: SUMMARY AND CONCLUSIONS

The bioactive glass with the composition of 45 SiO₂-23CaO (mol.%) was successfully synthesized by a melt quenching method. The attempt is made to investigate the effect of doping different concentration of Cr₂O₃ in the glass network. The characterization is carried out using XRD, FTIR, TGA and SEM spectroscopy of these samples. The techniques were utilized to characterize the samples with and without immersion in simulated body fluid. The glasses used in present study are:

1. 45% (SiO₂)-23% (CaO)-23% (NaO)-6% (P₂O₅)-3%-(SrO)-0%(CrO)
2. 44.95% (SiO₂)-23% (CaO)-23%(NaO)-6% (P₂O₅)-3%-(SrO)-0.05%(CrO)
3. 44.9% (SiO₂)-23% (CaO)-23% (NaO)-6% (P₂O₅)-3%-(SrO)-0.1%(CrO)
4. 44.7% (SiO₂)-23% (CaO)-23% (NaO)-6% (P₂O₅)-3%-(SrO)-0.3%(CrO)
5. 44.5% (SiO₂)-23% (CaO)-23% (NaO)-6% (P₂O₅)-3%-(SrO)-0.5%(CrO)
6. 44% (SiO₂)-23% (CaO)-23% (NaO)-6% (P₂O₅)-3%-(SrO)-1% (CrO)

The glasses were prepared by melt quenching method and the samples were characterized at room temperature. Following measurements were done:

1. The X-ray diffraction were recorded Rigaku Smart-lab diffractometer with incident CuK α (1.5406 Å) radiation source at 40 to 50kV at 40 mA. The data was collected in the angular range from 10° to 100° in a step size of 0.01° and measuring speed was set to 5° per min.
2. Infra-red absorption spectra for all six samples were obtained on a Shimadzu 8900 Infra-red Spectrometer in the wave number range 400 cm⁻¹ to 4000 cm⁻¹.
3. The Scanning electron microscope (SEM) micrographs were obtained at a magnification of 20,000 using the Joel SEM (EVO18).

4. The Scanning electron microscope (SEM) micrographs were obtained at a magnification of 20,000 using the Joel SEM (EVO18).

The main conclusions drawn from the results of above studies before and after immersion of glass samples in SBF are summarized below:

The densities of glass samples were found to be increased with concentration of chromium which was as expected, since the density of chromium oxide is at a higher scale. The obtained glass is a totally amorphous material with only broad diffuse hump around low angle region at around 31° for all the samples. The IR data on glasses without SBF confirmed that the glass former are the combination of Silicates and Phosphate. The bands observed were Si-O-Si symmetric bending is observed at around 490 cm^{-1} and 896 cm^{-1} corresponding to symmetric stretching is observed in all the glass samples. Si-O-Si, P-O, C-O and Sr-O bands were also observed in all the samples. As the concentration of CrO_2 increased the intensity of asymmetrical vibration is increased. The increase in chromium content does not show major changes in the glass structure. The glass transition temperature of all the glasses was found to be in the range of 535 to 580°C . SEM micrographs clearly showed the formation of hydroxyapatite layer on the surface. Elemental compositions obtained from EDS data. The *in vitro* experiment in SBF confirmed the bioactivity of glass by formation of apatite after 21 day which was confirmed by XRD and SEM data. These glasses can have potential application as in artificial bone substitute.

In future study once can test the mechanical flexural strength of these glasses and the *in vitro* studies on the glasses with incubation of the samples loaded with SBF in refrigeration for different cycles (1, 3, 5, 7, 14, 21, 36 days).

BIBLIOGRAPHY

1. Hench LL, West JK. Biological applications of bioactive glasses. *Life Chem Reports*. 1996;13:187–241.
2. Guarino, V.; Causa, F.; Ambrosio, L. Bioactive scaffolds for bone and ligament tissue. *Expert Rev. Med. Devices* **2007**, 4, 405-418.
3. Williams, D.F., proceedings of consequences conference of the European society for Biomaterials Chester, England March 3,5 1987
4. Hench LL, Xynos ID, Buttery LD, Polak JM. Bioactive materials to control cell cycle. *Mater Res Innovations*. 2000;3:313–23.
5. Ylanen H., Karlsson K.H., Itala A., Aro H.T.: *J. Non- Cryst. Solids* 275, 107 (2000)
6. Introduction to solid state physics by Charles Kittel.
7. <https://link.springer.com/article/10.1007/s120>
8. <https://en.wikipedia.org/wiki/Glass>
9. https://shodhganga.inflibnet.ac.in:8443/jspui/pdfToThesis.jsp?toHandle=https://shodhganga.inflibnet.ac.in/handle/10603/25204&toFile=https://shodhganga.inflibnet.ac.in/bitstream/10603/25204/8/08_chapter%201.pdf
10. https://www.lehigh.edu/imi/teched/AtModel/Lecture_2_Micoulaut_Atomistics_Glass_Course.pdf
11. https://www.researchgate.net/figure/Schematic-phase-diagram-of-a-glass-former-in-the-vicinity-of-the-glass-transition-The_fig1_275335055
12. https://www.google.com/search?q=vitrification&rlz=1C1VDKB_enIN979IN979&oq=vvitrification&aqs=chrome..69i57.8408j0j7&sourceid=chrome&ie=UTF-8
13. http://shodhganga.inflibnet.ac.in/bitstream/10603/25204/8/08_chapter%201.pdf
[Chapter 1: Introduction (1.6.1)]

14. https://scholar.google.co.in/scholar?q=larry+hench+work+on+bioactive+glass&hl=en&as_sdt=0&as_vis=1&oi=scholar
15. http://shodhganga.inflibnet.ac.in/bitstream/10603/29808/9/09_chapter%201.pdf
16. [Chapter 1: Introduction (General concepts of glasses 1.2-1.3)]
17. http://shodhganga.inflibnet.ac.in/bitstream/10603/25204/8/08_chapter%201.pdf
[Chapter 1: Introduction (1.6.1)]
18. <http://shodhganga.inflibnet.ac.in/bitstream/10603/11891/5/06-chapter%201.pdf>
19. [Fundamental of glasses: Chapter 1 (1.2.2)]
20. <https://www.thequartzcorp.com/2019/09/23/the-mechanism-of-bioactive-glass/>
21. https://www.wikiwand.com/en/Bioactive_glass
22. <https://www.thequartzcorp.com/2019/09/23/the-mechanism-of-bioactive-glass/>
23. T. Kokubo, H. Kushitani, S. Sakka, T. Kitsugi and T. Yamamuro, "Solutions able to reproduce in vivo surface-structure changes in bioactive glass-ceramic A-W", J. Biomed. Mater. Res., 24, 721-734 (1990).
24. <https://www.sciencedirect.com/science/article/abs/pii/S0144861709003713>
25. https://repository.upenn.edu/xray_scattering_intro/3/
26. SEM manual(basic knowledge of using the sem) by Joel
27. EVO user manual
28. Fourier transform infrared spectroscopy: applications to chemical systems / edited by John R. Ferraro, Louis J. Basile ; contributors, Louis J. Basile ... et al.
29. A. Paul, Chemistry of glasses, (Chapman and Hall, London, 1982)
30. S. R. Elliot, Physics of Amorphous materials, (Longman, London 1990).